香港氣象學會

HONG KONG METEOROLOGICAL SOCIETY

Bulletin

VOLUME 7, NUMBER 1, 1997
ISSN: 1024-4468

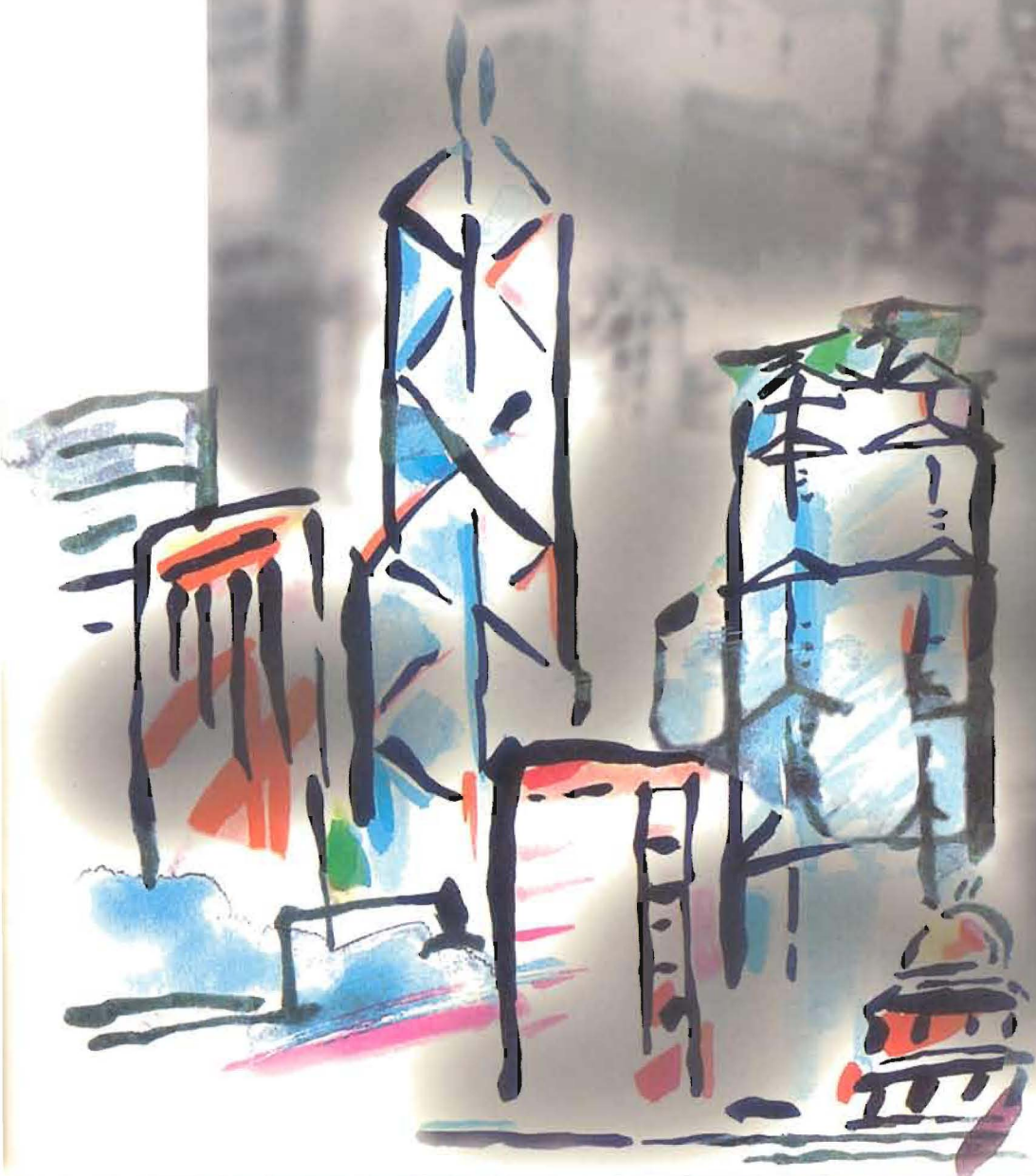

ISSN 1024-4468

The **HONG KONG METEOROLOGICAL SOCIETY BULLETIN** is the official organ of the Society, devoted to articles, editorials, news and views, activities and announcements of the Society.

Members are encouraged to send any articles, media items or information for publication in the **BULLETIN**. For guidance see the "**INFORMATION FOR CONTRIBUTORS**" in the inside back cover.

Advertisements for products and/or services of interest to members of the Society are accepted for publication in the **BULLETIN**.

For information on formats and rates please contact the Society secretary at the address opposite.

Views and opinions expressed in the articles or any correspondence are those of the author(s) alone and do not necessarily represent the views and opinions of the Society.

The mention of specific products and/or companies does not imply there is any endorsement by the Society or its office bearers in preference to others which are not so mentioned.

SUBSCRIPTION RATES (Two issues per volume)

Institutional rate: HK$ 300 per volume

Individual rate: HK$ 150 per volume

Published by

The Hong Kong Meteorological Society

c/o Hong Kong Observatory
134A Nathan Road
Kowloon, Hong Kong

香港氣象學會

HONG KONG METEOROLOGICAL SOCIETY

Bulletin

VOLUME 7, NUMBER 1, 1997

CONTENTS

Editorial

This issue of the **BULLETIN** contains two papers whose results provide useful information related to important issues such as aviation and marine safety as well as aspects of the continuing increase in air pollution affecting Hong Kong. One is concerned with long-term visibility trends while the other reports on numerical modelling of the sea-land breeze system.

The first paper by C.M. Cheng, C.C. Chan and S.T. Chan of the Hong Kong Observatory, reports on a long-term study of visibility trends at two urban stations and two outlying island stations. The results suggest a long-term increasing trend indicating a decline in visual air quality although there was, as might be expected, considerable spatial and temporal variation attributable to meteorological variations in airflow velocity and direction.

In the second paper, Zhang Ming and Zhang Lifeng of the Institute of Atmospheric Physics, Chinese Academy of Sciences report on research which they undertook while at the Department of Physics, The Chinese University of Hong Kong. This research, supported in part by a grant from the Croucher Foundation, studied the land-sea breeze system in Hong Kong using a modified Mass model incorporating the effects of large-scale background air flow, localized urban heating and the differential heating of sun-facing mountain slopes. The results from the model were compared with an analysis of meteorological data over a ten-year period and agree well with observations. As a consequence the authors believe that the results of the study should be useful for weather forecasting, aviation safety and understanding airborne pollutant dispersal in Hong Kong.

The remainder of the issue contains the regular features *News and Announcements* and *Hong Kong Weather Reviews.*

The Editorial Board, as always, look forward to receiving any opinions, suggestions or contributions sent in by readers.

Bill Kyle, Editor-in-Chief

C.M. Cheng, C.C. Chan and S.T. Chan

Hong Kong Observatory, 134A Nathan Road, Hong Kong

Visibility Trends in Hong Kong

1. Introduction

Forecasters at the Observatory have noticed in the last few years that during the onset of surges of the northeast monsoon, meteorological visibility inside Victoria Harbour apparently deteriorated to a greater extent than in the past. As visibility is often treated as an indicator of visual air quality (Sloane, 1982), the trend of reduction in visibility, if genuine, would be of interest.

Chang and Koo (1986) investigated the variation in visibility in Hong Kong from 1968 to 1982. In their investigation, occurrences of visibility reduction not due to meteorological phenomena such as fog, mist, precipitation and high humidity (95 percent or above) had a statistically significant upward trend during the period 1975 to 1980.

The aim of the present study is to investigate the annual variation in reduced visibility in Hong Kong from 1968 to 1995 with a view to finding out whether there were trends in visibility. A few cases of visibility degradation will also be analyzed to help appreciate the relationship between meteorological conditions and degraded visibility.

2. Data Base

Visibility observations at four stations in Hong Kong were analyzed. The locations of the four stations, namely the Hong Kong Observatory (HKO), Hong Kong International Airport (HKIA), Cheung Chau (CC) and Waglan Island (WI), are shown in Figure 1. HKO and HKIA are located in the urban area by the side of the Victoria Harbour. CC and WI are outlying islands situated over the southwestern and southeastern side of the territory respectively. Table 1 lists the period and frequency of visibility observations at these stations.

In order to focus on the change in visual air quality, it is necessary to screen out the effect of weather from the visibility data. To do this, the present investigation has followed Chang and Koo's (1986) procedure, that is, excluding cases of visibility impairment that were concurrent

with reports of fog, mist, precipitation, or relative humidity of 95 percent or above from the visibility data. In general, visibility is said to have been reduced when it falls below 8 km. Hence, "reduced visibility" here refers to visibility below 8 km when no fog, mist, precipitation or relative humidity of 95 percent or above are reported.

Figure 1. Location in Hong Kong of four stations used for study of visibility data

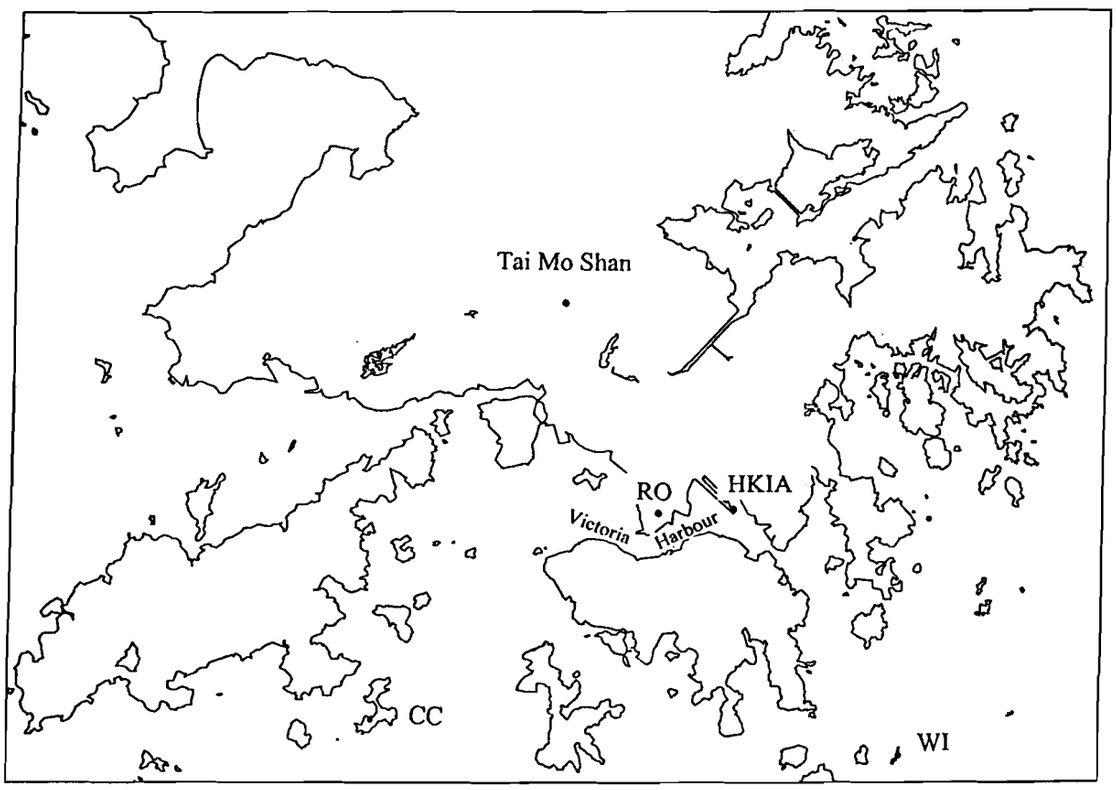

Table 1. Base data of visibility observations (HKO - Hong Kong Observatory, HKIA - Hong Kong International Airport, CC - Cheung Chau, WI - Waglan Island)

	HKO	*HKIA*	*CC*	*WI*
Time period	1968-1995	1968-1995	1968-1991*	1975-1988*
Frequency of data	hourly data	hourly data	hourly data	3 hourly data

* manual observations of visibility are not available at CC and WI after these dates

The number of hours of reduced visibility at each station was counted. To facilitate comparison, the annual or monthly number of hours of reduced visibility at each station were expressed as a percentage of the total number of hours that observations were made at that station in that year or month. These percentages were analyzed to see if any trend exists.

3. Year-to-year Variations in Reduced Visibility

Figure 2 illustrates the year-to-year variations of reduced visibility at the four stations. To minimize inter-annual variations so as to reveal the long term trend, smoothing of the curves was done by computing the running 3-yearly means of the annual frequency of reduced visibility and the results are also plotted in the same figure.

Figure 2. Annual percentage of reduced visibility (solid line) and their running 3-year mean (dashed line) for each of the four stations

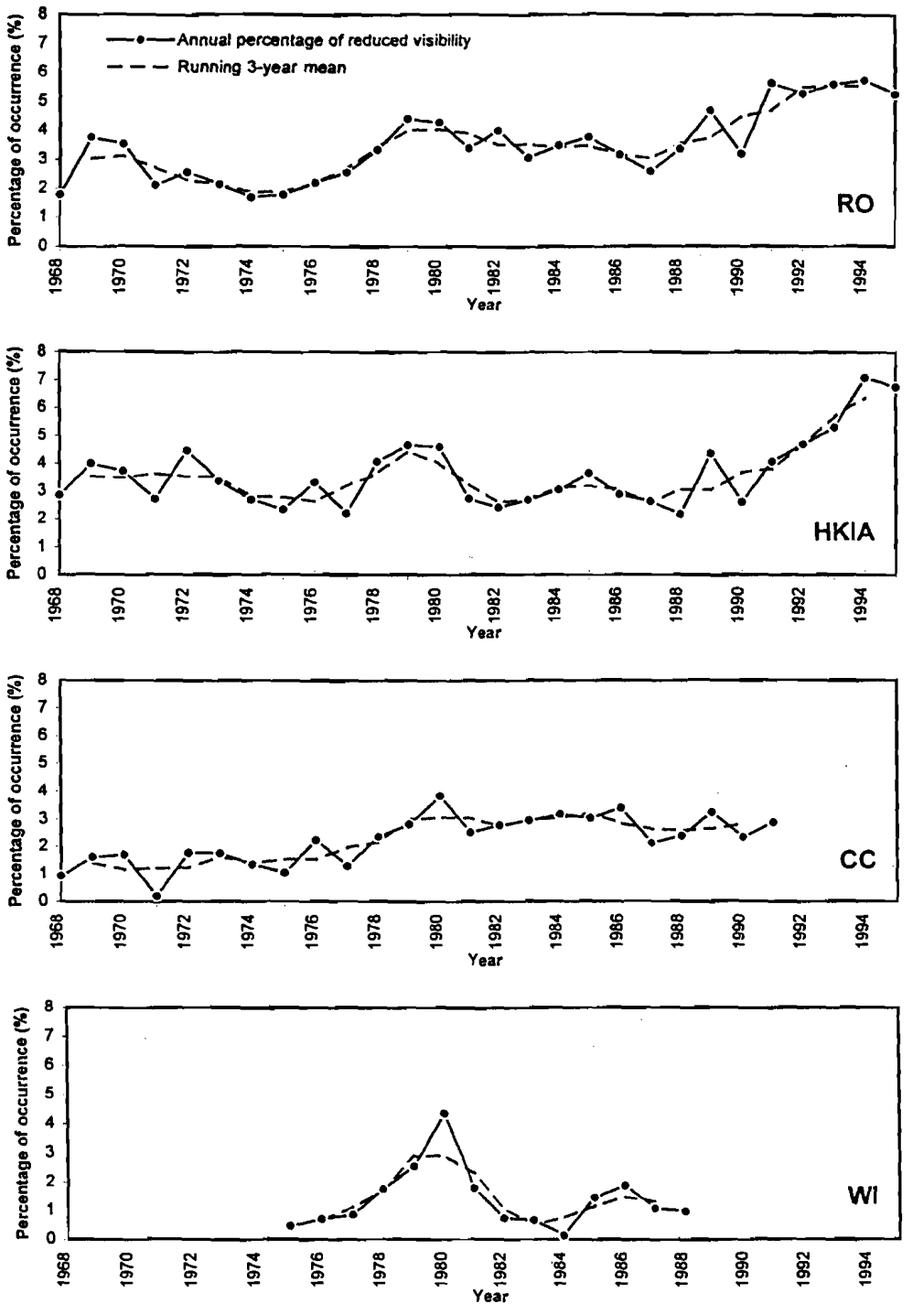

From Figure 2, it can be seen that the running means of HKO and HKIA showed a decreasing trend before 1975 while CC experienced a weak increasing trend during that time. However, all four stations had a noticeable increasing trend from 1975 to 1979. This is similar to the findings of Chang and Koo (1986).

From 1979 onwards, the variation in the running means of CC was small and if anything showed a very weak decreasing trend. In WI, however, the percentage figure fell to a minimum in 1984. It then increased again till the late 1980s when manual observation ceased. At HKO, the curve showed that the percentage of reduced visibility experienced a decreasing trend from 1979 to 1987. This period with decreasing trend was much shorter at HKIA, lasting only from 1979 to 1982. The variation from 1982 to 1987 was relatively small at HKIA. From 1987 onwards, both HKO and HKIA showed a significant increasing trend. The trends of reduced visibility at the four stations are summarized in Table 2.

Table 2. Year-to-year variations in percentage of reduced visibility at the 4 stations.

Period	*Before 1975*	*1975-1979*	*1979-1983*	*1983-1987*	*1987 onwards*
HKO	decreasing	increasing	decreasing	decreasing	increasing
HKIA	decreasing	increasing	decreasing	small	increasing
CC	increasing	increasing	small	small	small
WI	-	increasing	decreasing	increasing	-

From the discussion above, rising and falling trends of reduced visibility at a time frame of roughly 5 years were observed at each station even from curves of running 3-yearly means. It is therefore difficult to determine from these curves long term trends for the entire period under study. To establish this long term trend, two methods were employed. Firstly, fluctuations with cycles of about 11 years (Figure 2) were observed in the reduced visibility data. These fluctuations were removed by applying a 11-year Gaussian filter. The long term trend was then assessed from the filtered data. While this method is mathematically rigorous, it suffers from the fact that trends for the first 5 years as well as the last 5 years of the period under study cannot be determined. The second method employed fitting of straight lines to the reduced visibility data for each station using least squares. The long term trend could then be inferred from the slopes of these straight lines.

After applying the 11-year Gaussian filter, the resultant reduced visibility data are plotted in Figure 3. The curve for WI is too short to infer any meaningful trend. It is, however, rather obvious that frequency of reduced visibility at HKO was rising steadily. The variation of reduced visibility at HKIA was small in the long term but the rising trend after 1987 mentioned above managed to manifest itself in the filtered data. The long term trend for CC was also rising but it seemed to level off after 1981.

Results obtained using the second method are shown in Figure 4. Table 3a presents the results of the least square fitting. Among the four stations, reduced visibility at WI experienced a large fluctuation and no statistically significant trend could be inferred for it. Reduced visibility at HKO and CC both exhibited a statistically significant rising trend with overall significance (by F

test) at the 1% level. The rate of rise were 0.11% and 0.09% per year at HKO and CC respectively. For HKIA, although the slope of the best fitted straight line is positive, indicating a rising trend of 0.07% per year, this trend is not significant at the 1% level (by F test).

Figure 3. Annual percentage of reduced visibility (solid line) the running 11-year Gaussian filtered annual percentage of reduced visibility (dashed line) for the four stations

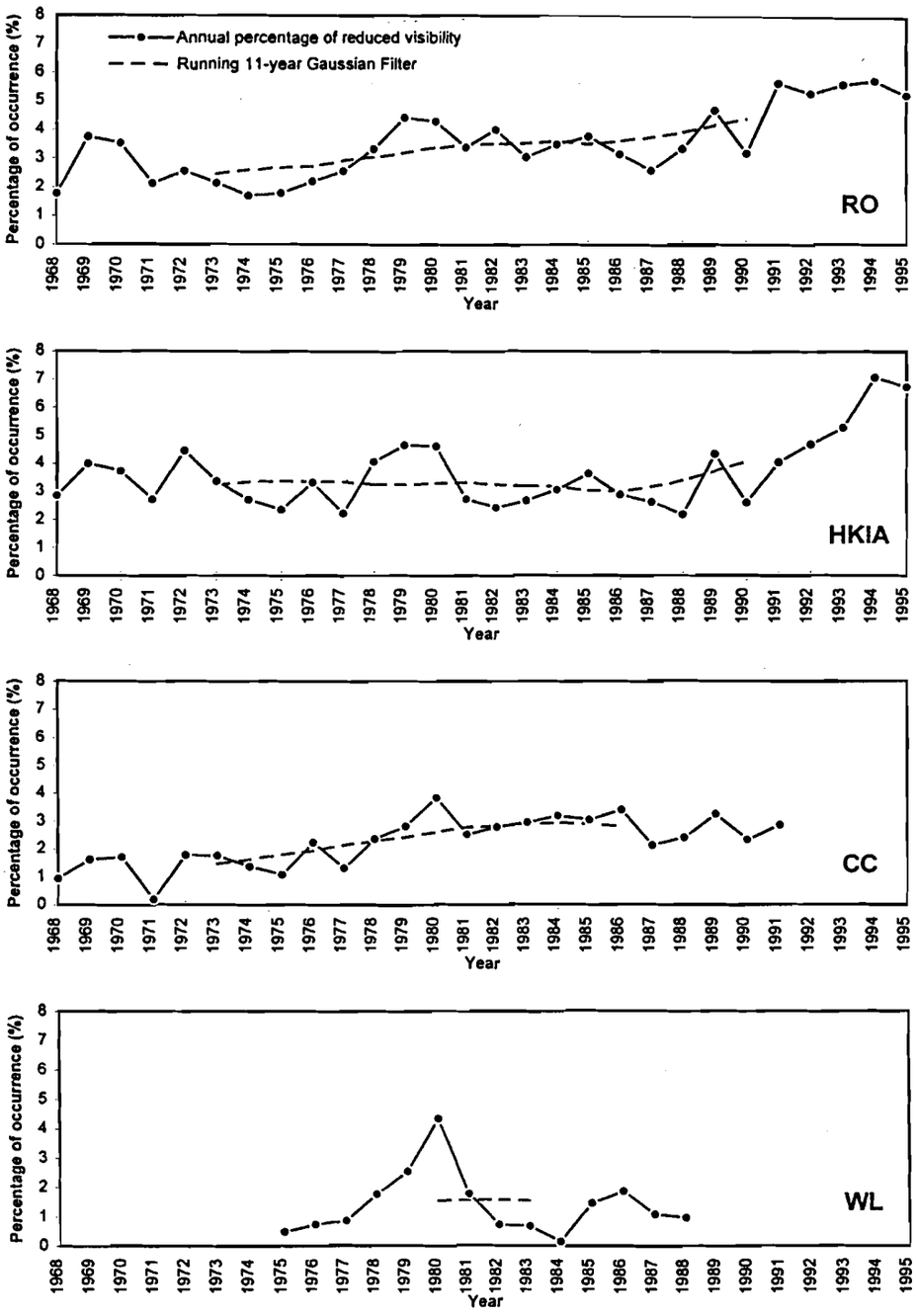

Thus the results of both methods indicate that for the period 1968 to 1995 as a whole, reduced visibility at HKO and CC had a significant long term rising trend. For HKIA, while there was no statistically significant long term trend, the results hint at an increasing trend in recent years.

Figure 4 (a). Annual percentage of reduced visibility (solid line) and the best fitting straight line by linear regression (dashed line) for the four stations

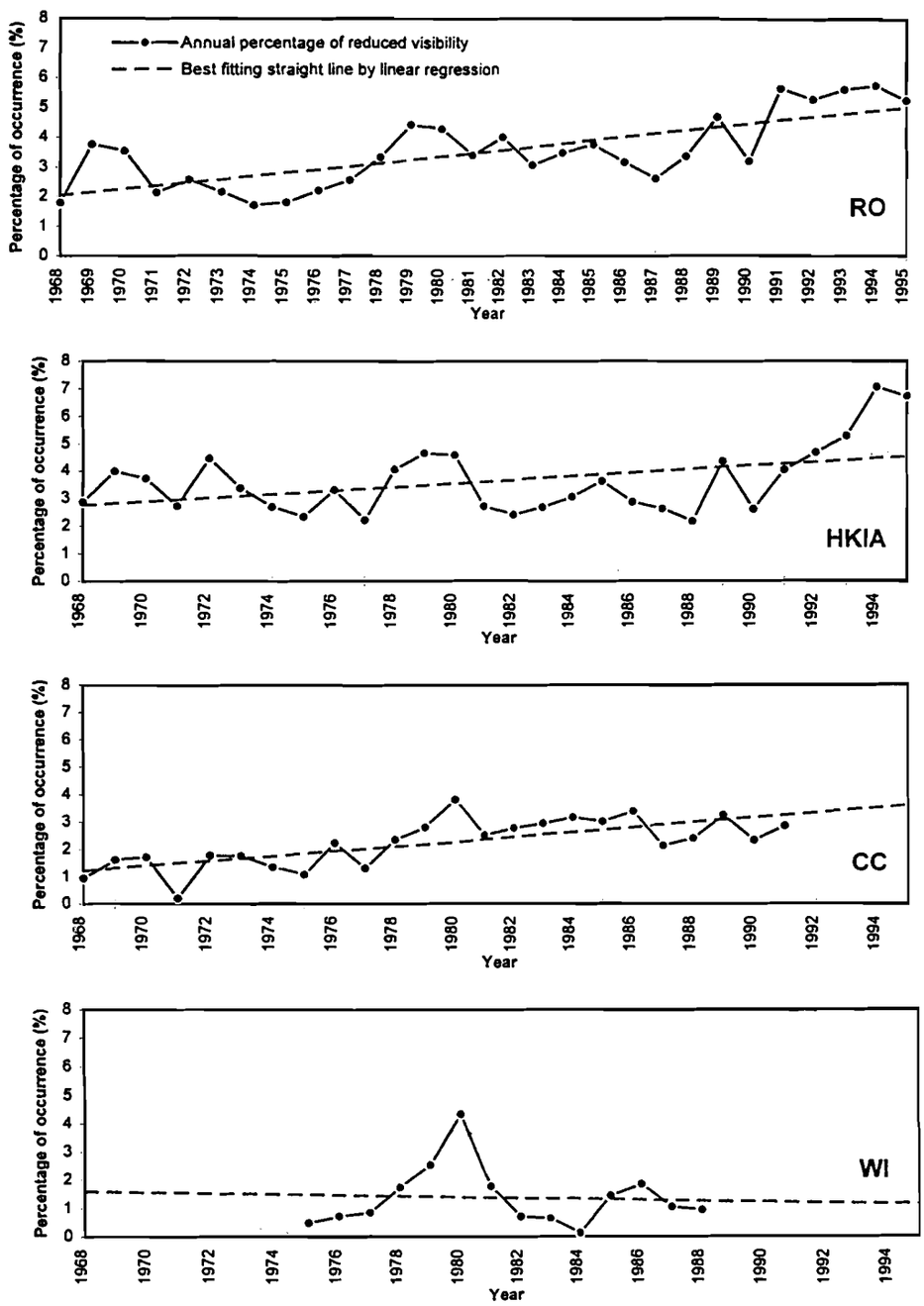

Figure 4 (b). Same as Figure 4 (a) except for the period 1987 to 1995 at HKO and HKIA

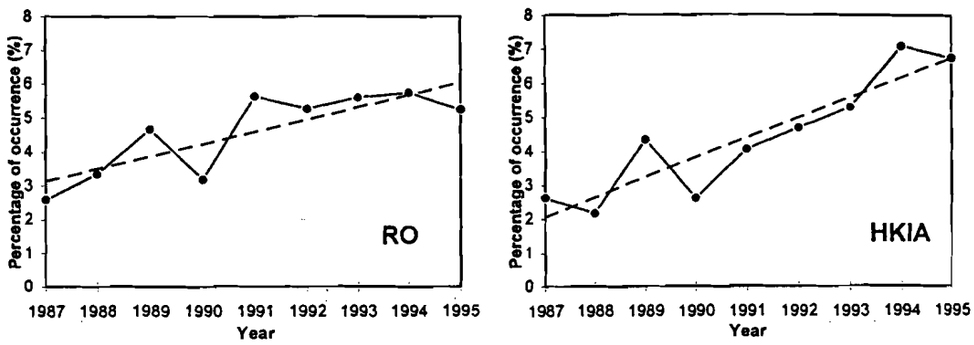

Table 3(a). Linear fit of annual percentage of reduced visibility at the four stations

Station	*Intercept a*	*Slope b*	*y = a + bt*	*y is moving average centred on*	*95% confidence limits for b*	*Coefficient of determination r^2*	*Overall significance by F test*
HKO (1968-1995)	1.92	+0.11	y = 1.92 + 0.11 t	1967 + t, t=1,2, ., 28	+0.07 to +0.15	0.54	1%
HKIA (1968-1995)	2.69	+0.07	y = 2.69 + 0.07 t	1967 + t, t=1,2, ., 28	+0.01 to +0.12	0.18	Insignificant at 1%
CC (1968-1991)	1.13	+0.09	y = 1.03 + 0.09 t	1967 + t, t=1,2, ., 24	+0.05 to +0.13	0.50	1%
WI (1968-1988)	1.50	-0.02	y = 1.50 - 0.02 t	1974 + t, t=1,2,., 14	-0.18 to +0.14	0.00	Insignificant at 1%

Table 3(b). same as Table 3(a) except for the period 1987 to 1995 at HKO and HKIA

Station	*Intercept a*	*Slope b*	*y = a + bt*	*y is moving average centred on*	*95% confidence limits for b*	*Coefficient of determination r^2*	*Overall significance by F test*
HKO	2.78	+0.36	y = 2.78 + 0.36 t	1986 + t, t=1,2, ., 9	+0.13 to +0.59	0.66	1%
HKIA	1.47	+0.58	y = 1.47 + 0.58 t	1986 + t, t=1,2,., 9	+0.34 to +0.83	0.82	1%

As mentioned earlier, reduced visibility at HKO and HKIA has shown a noticeable rising trend since 1987. To compare the rate of increase since 1987 with the long term rate, straight lines are also fitted by linear regression to the reduced visibility data from 1987 to 1995 for HKO and HKIA (Table 3b). The rate of increase at HKO during this period was 0.36 percent per year, more than 3 times higher than the long term rate. The increase in rate was even more pronounced at HKIA, which showed a value of 0.58 percent per year. Visual inspection of the HKO curve in Figure 4a suggests that the rapid increase might be the result of a combination of the long-term increasing trend and the rising segment of a quasi-periodic fluctuation with a decadal time scale. The HKIA curve in Figure 4a also shows similar characteristics.

To test the notion of degradation of visibility during onset of surges of the northeast monsoon, the trends for reduced visibility in autumn/winter were also studied. Here, autumn/winter is taken as the period from 16 September to the end of February of the following year. This is the period when surges of the northeast monsoon come to affect Hong Kong from time to time. Reduced visibility data for this period were analyzed with the same methods that were applied to the data for the whole year. The trends for reduced visibility in autumn/winter and trends for annual reduced visibility resemble each other rather closely. Results are therefore not presented here.

4. Effect of Wind Direction on Reduced Visibility

To study the effect of wind direction on reduced visibility, a wind rose was constructed for all cases of reduced visibility at HKO from 1968 to 1995. This wind rose is shown in Figure 5 together with the climatological mean wind rose. Thus reduced visibility occurs predominantly in easterly and westerly winds. Let R be the frequency of a wind direction in the wind rose for reduced visibility and C be the corresponding climatological value. Table 4 lists out the values of R and C for different wind directions. For cases of reduced visibility, the proportion of winds from the west, i.e. R, is 16%. The climatological frequency of westerly winds, i.e. C, is however a low 8%. The ratio R/C amounts to 2 and is significantly higher than the ratios for other wind directions. It therefore follows that westerly winds at HKO are associated with a higher probability of reduced visibility than other wind directions.

Figure 5. (a) Wind rose for reduced visibility at HKO from 1968 to 1995
(b) Climatological wind rose for HKO from 1961 to 1990

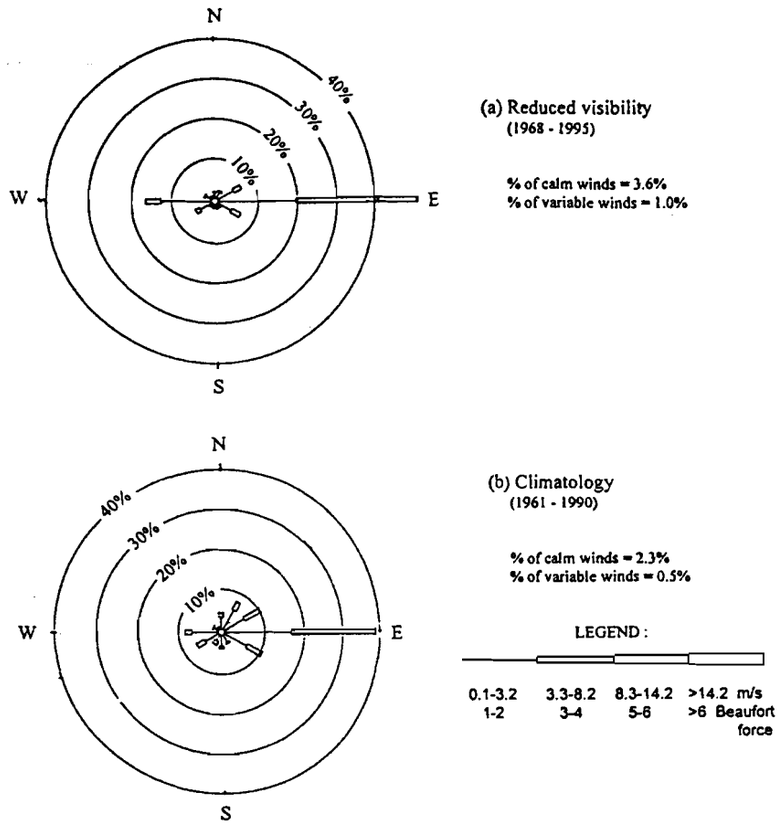

It is well known to forecasters in Hong Kong that because of the local terrain, when the prevailing wind is light northerly, HKO very often records westerly winds. The above statistics suggest that the chance of reduced visibility at HKO is higher under a northerly airstream. In this connection, it is interesting to note that previous work by Bell (1970) showed that the Gobi Desert and other arid areas of China are sources of fine particles to Hong Kong.

Table 4. Differences between the climatological wind rose and the wind rose for reduced visibility at HKO

	Climatological wind rose (C) (1961-1990)	*Wind rose for reduced visibility (R) (1968-1995)*	*R/C*
Frequency of easterly winds	39%	51%	1.3
Frequency of westerly winds	8%	16%	2
Frequency of winds from other directions	53%	33%	0.6

5. Cases of Reduced Visibility

In order to study how various factors affect visibility, the meteorological conditions of a few cases of reduced visibility were analyzed and the results are given below.

(a) Weak northerly surge on 20 December 1990

On 19 December 1990, a ridge of high pressure lay along southeast China, bringing an easterly airstream to the coast of Guangdong (Figure 6). This ridge of high pressure weakened the next day as another ridge built up over western China. A weak northerly surge associated with the latter ridge arrived at the coast of Guangdong that day and replaced the prevailing easterly airflow. Figure 7 illustrates the changes in wind field in Hong Kong on 20 and 21 December 1990 as recorded by a network of automatic weather stations (AWS). At 10 a.m. HKT on 20 December (Figure 7a), winds in Hong Kong were mostly light. Northerly winds associated with the weak surge had already reached the northern part of the territory. An east-west line of wind convergence between northerlies in the north and south to southeasterlies to the south was clearly discernible. At this time, winds at HKO was light easterly while visibility at HKO and HKIA was 9 and 8 km respectively (Figure 8).

By noon, winds at HKO had turned light westerly and visibility fell slightly to 7 km. Visibility at HKIA was still 8 km. A closer look at the wind field at 2 p.m. HKT (Figure 7b) indicated that the westerly winds at HKO was a result of the southward penetration of northerly winds associated with the surge and the southeast drift of the line of wind convergence to the Victoria Harbour. By this time, winds over the western part of Hong Kong turned into northwesterlies and westerly winds at HKO reached 4 ms^{-1}. At 6 p.m. HKT (Figure 7c), winds over the northwestern part of the territory had strengthened but wind convergence was still observable between HKO and HKIA. At this time, both HKO and HKIA recorded the lowest visibility of 3200 and 3500 m respectively.

Figure 6. Synoptic weather maps for 2 a.m. HKT on 19 and 20 December 1990.

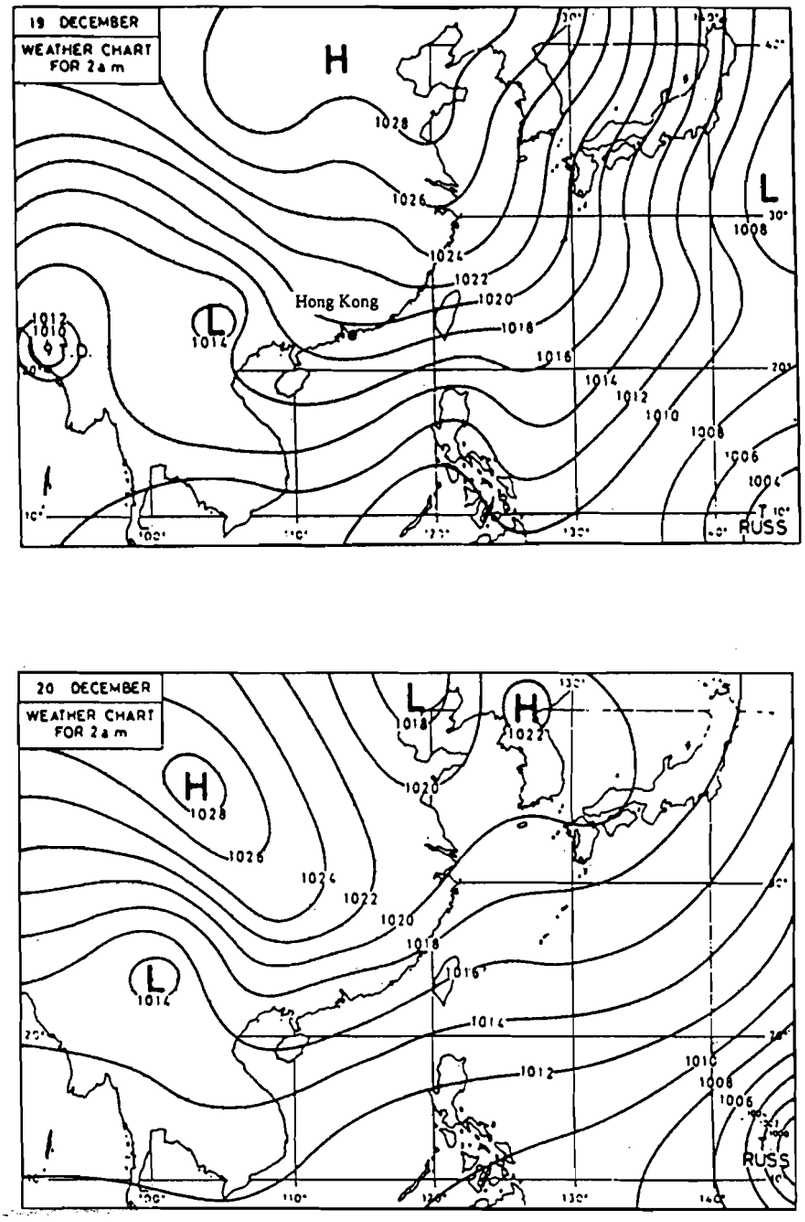

Figure 7. Wind flow over Hong Kong (a) at 10 a.m. HKT on 20 December 1990, (b) at 2 p.m. HKT on 20 December 1990, (c) at 6 p.m. HKT on 20 December 1990 and (d) at 2 a.m. HKT on 21 December 1990

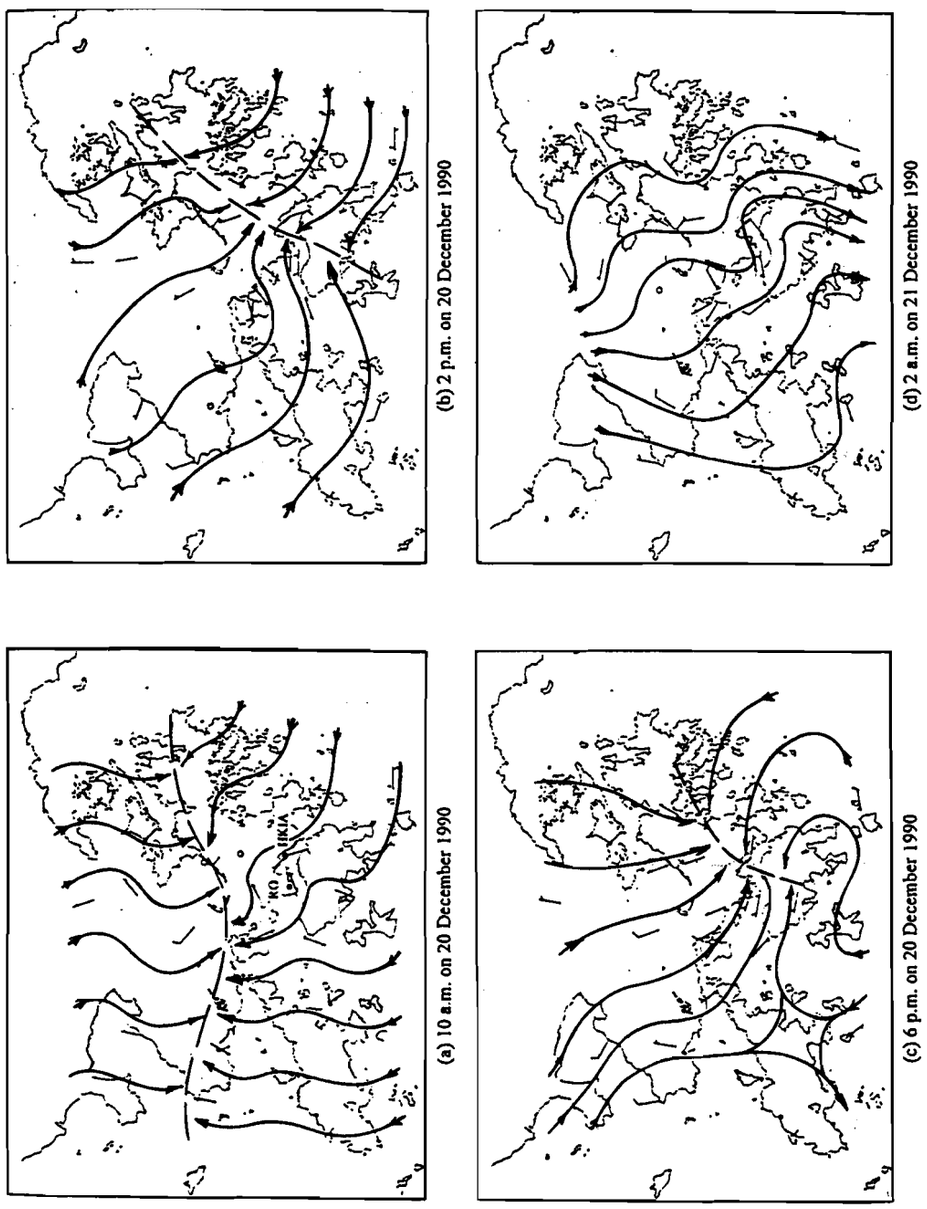

Figure 8. Wind at HKO, visibility at HKO and HKIA from 8 a.m. HKT on 20 December 1990 to 7 a.m. HKT on 21 December 1990

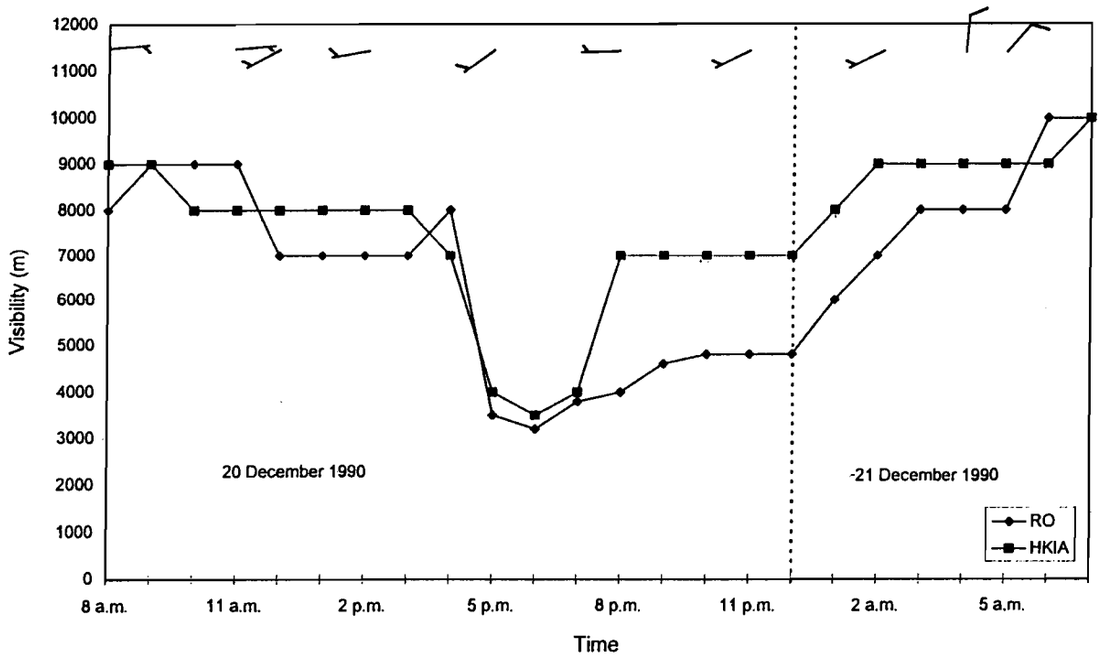

Visibility at both stations remained 7 km or below for the next few hours but gradually improved after midnight. At 2 a.m. HKT on 21 December 1990 (Figure 7d), the convergence of winds within Hong Kong ceased to exist. Visibility at HKO and HKIA gradually improved in the next few hours and reached 10 km and 9 km respectively by 6 a.m. HKT.

From this analysis of AWS data, the arrival of the weak northerly surge was accompanied by a line of wind convergence. Accumulation of suspended particles was favoured in the vicinity of this line of convergence. Soon after its passage and the subsequent strengthening of winds, visibility improved generally.

(b) Lull in winter monsoon on 8 January 1994

Figure 9 depicts the synoptic situation for 7 and 8 January 1994. A ridge of high pressure along the coast of southeast China brought an easterly airstream to Hong Kong on 7 January 1994. With the weakening of this ridge, winds in Hong Kong subsided the next day. The wind flow and temperatures in Hong Kong on 8 January are shown in Figure 10. Early on 8 January 1994 (Figure 10a), moderate easterly winds prevailed inside the Victoria Harbour. Visibility at HKO and HKIA was 7 km and 8 km respectively (Figure 11) while temperatures in the territory ranged between 16 to 18 degrees Celsius.

Visibility at HKO fell to 4800 m at 7 a.m. HKT and remained low for the next 12 hours or so. The visibility at HKIA, however, remained at around 7-8 km until noon. The local conditions at 10 a.m. HKT (Figure 10b) might explain the deterioration in visibility at HKO. It was found that winds inside the Victoria Harbour dropped while weak northerly winds invaded the northern part of the territory. On checking the synoptic conditions, it was found that the air pressure was generally falling at that time in the territory while the dew point was

Figure 9. Synoptic weather maps for 2 a.m. HKT on 7 and 8 January 1994.

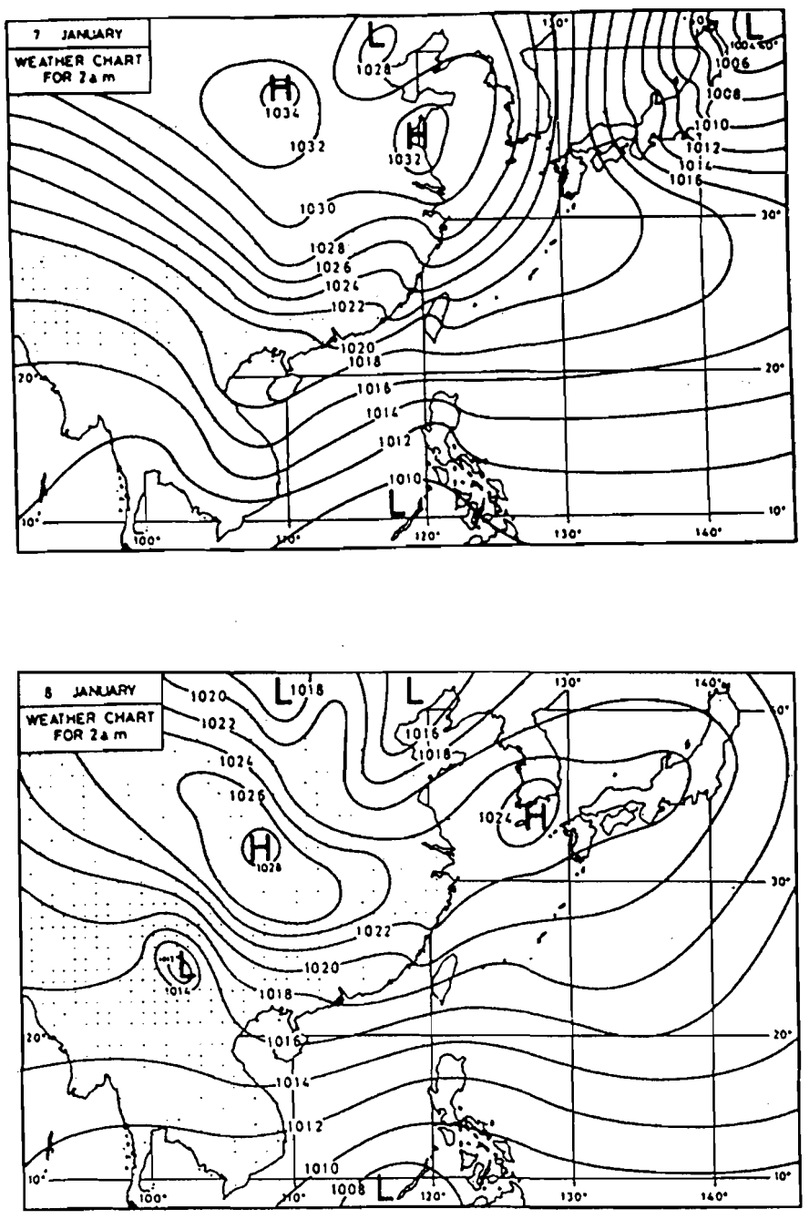

Figure 10. Wind flow and temperatures over Hong Kong (a) at midnight HKT early on 8 January 1994, (b) at 10 a.m. HKT on 8 January 1994, (c) at 1 p.m. HKT on 8 January 1994 and (d) at 8 p.m. HKT on 8 January 1994

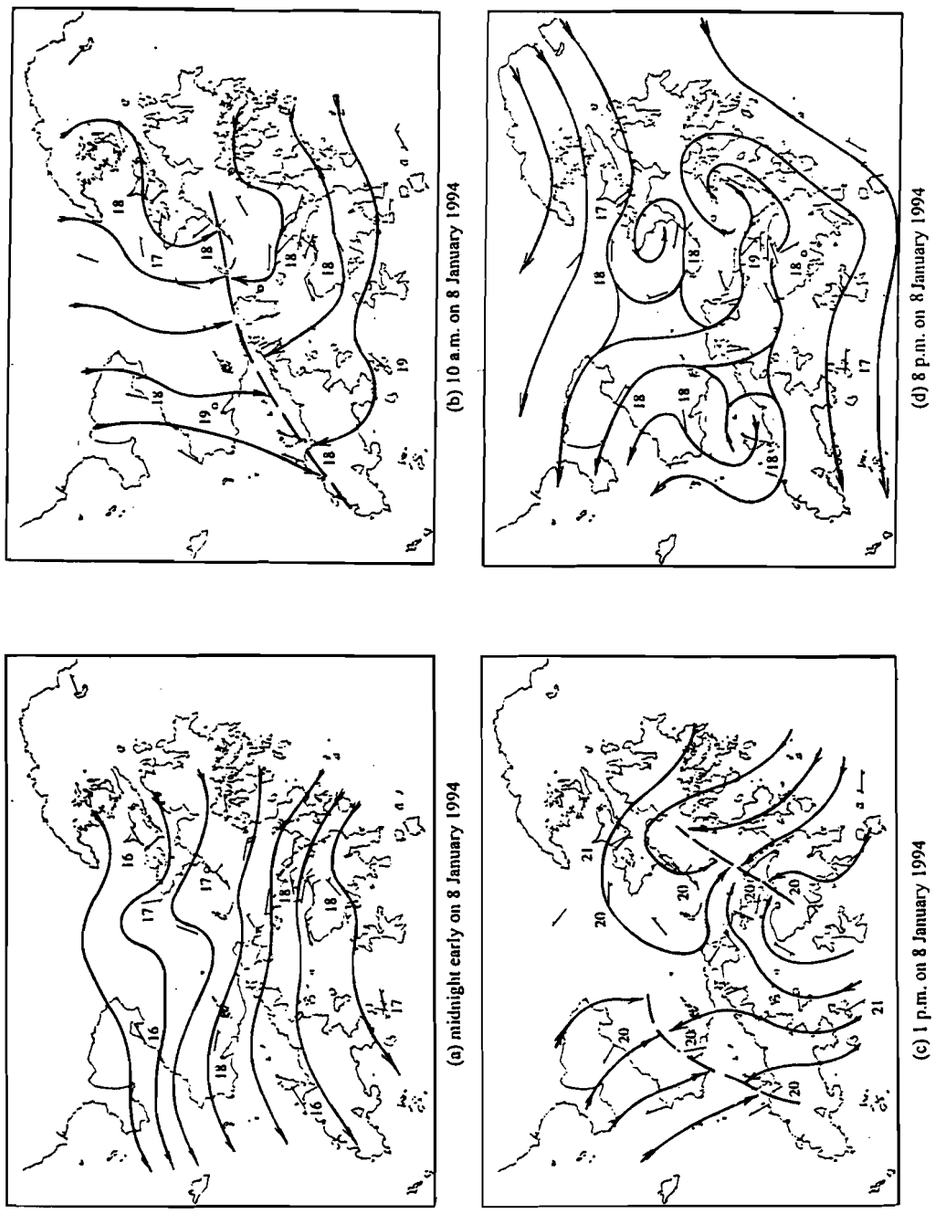

Figure 11. Wind at HKO, visibility at HKO and HKIA from 1 a.m. HKT on 8 January 1994 to 3 a.m. HKT on 9 January 1994

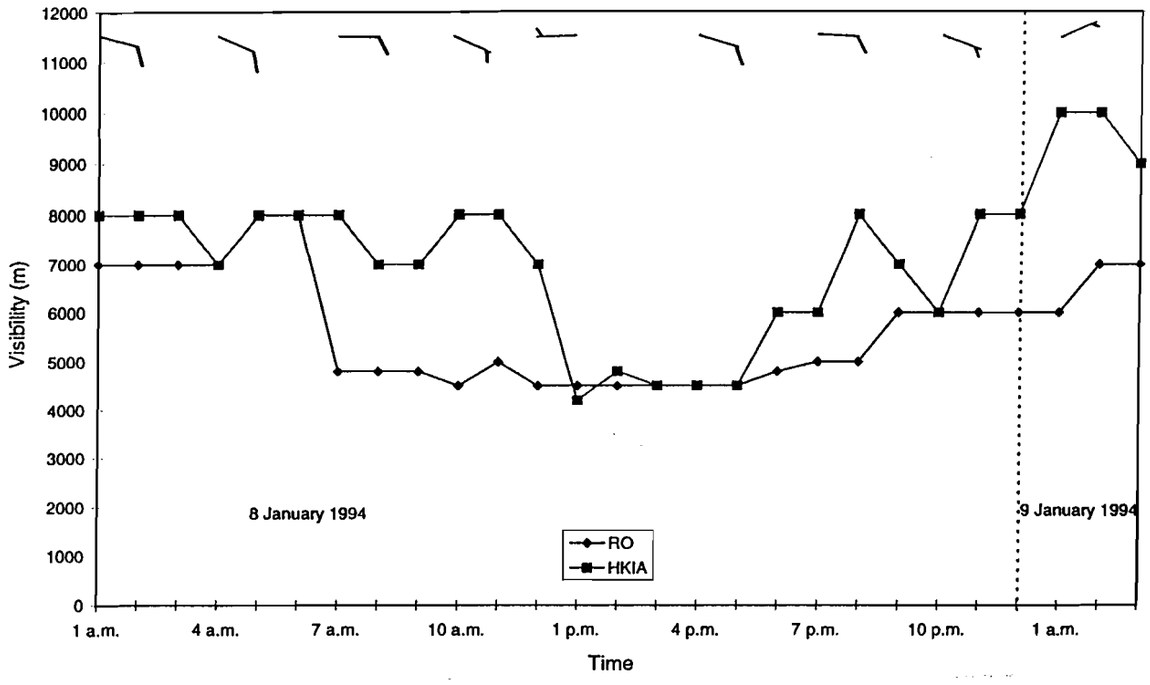

hardly changing at all. It was concluded that these northeasterly winds were not due to the arrival of a surge of the northeast monsoon. Noting that temperatures in the northwestern part of the New Territories rose to 18 to 19 degrees Celsius by 10 a.m. HKT and that the sea surface temperature was 18 degrees Celsius on that day, sea breezes could have set in by this time. Because of the orientation of coastline, sea breezes in the northwestern part of the New Territories had northerly components.

At this time, a line of convergence between the north and easterly winds could be seen lying across the territory. Winds at both HKO and HKIA had abated to 3 ms^{-1} and 1 ms^{-1} respectively. Visibility at HKO dropped to 4500 m. By 1 p.m. HKT (Figure 10c), temperatures within Hong Kong rose to 20 degrees Celsius in general. Sea breezes acquired their full strength and winds over the northwestern part of the New Territories and Lantau Island turned northwesterly. Sea breezes had also set into the Victoria Harbour. Because of the geometric configuration of the Kowloon Peninsula, sea breezes at the HKIA were southeasterly while those at the HKO were westerly. Because of the influence of sea breezes, the wind flow over the territory was weak and complicated. Two lines of wind convergence could now be analyzed. One of them was located in the western part of the territory while the other one lay between HKO and HKIA. Visibility at this time was down to 4500 m at HKO and 4200 m at HKIA, and remained low for the next several hours.

By 8 p.m. HKT (Figure 10d), temperatures fell to 17 to 18 degrees Celsius generally and easterly winds re-established themselves again over the territory. Visibility at HKO and HKIA improved to 5 km and 8 km respectively. This case indicates that weakening of winds during lulls in the winter monsoon favours the setting in of sea breezes. Because of the complicated geometry of the coastline, lines of convergence exist between these sea breezes. It is near these lines of convergence that visibility degradation might occur.

(c) Pre-tropical cyclone situation on 17 August 1990

At 2 a.m. HKT on 16 August 1990, Severe Tropical Storm Yancy was located about 700 km southeast of Taiwan (Figure 12). While Yancy travelled northwestward towards Taiwan, its outer circulation started to affect Guangdong the next day. From AWS winds (Figure 13), it was observed that winds were rather irregular in Hong Kong at 8 p.m. HKT on 16 August (Figure 13a) because of the presence of some thundery activity. Winds at Tai Mo Shan were moderate from the northeast. Visibility at both HKO and HKIA was 10 km or above (Figure 14).

By 6 a.m. HKT the next morning (Figure 13b), Hong Kong came under the influence of the outer circulation of Yancy. Winds at Tai Mo Shan turned to the northwest and organized west to northwesterly winds dominated the territory. Visibility at HKO and HKIA was still good at this time. As the west to northwesterly winds continued to prevail, visibility gradually decreased. At 4 p.m. HKT on 17 August 1990 (Figure 13c), visibility at HKO and HKIA was down to 3000 m and 4000 m respectively while winds at both stations were 4 ms^{-1}. At that time visibility at both stations varied between 4000 m and 7 km. At midnight HKT late on 17 August (Figure 13d), winds turned northerly generally. Winds at HKIA increased to 7 m/s and visibility there rose to 10 km. Since HKO is sheltered from the north by mountains, winds there were calm at this time. Visibility, nevertheless, soared to 7 km and further improved in the next few hours.

Because of the subsidence of air on the outer periphery of Yancy, the atmosphere was rather stable and was conducive to the occurrence of reduced visibility associated with dust trapped in the lower atmosphere. In this case, no apparent line of wind convergence could be observed. Nevertheless, a drop in visibility was accompanied by the setting in of northwesterly winds.

6. Conclusions

Visibility data for two urban stations (28 years) and two outlying island stations (over 10 years) were studied. Results indicate that trends for annual and winter reduced visibility resemble each other closely. Reduced visibility had statistically significant upward trends at HKO and CC while no statistically significant trend could be inferred for HKIA. Moreover, both HKO and HKIA exhibited a high rate of increase in the frequency of reduced visibility between 1987 and 1995. This may be related to the superposition of a quasi-periodic fluctuation with a decadal time scale on top of a long-term increasing trend.

It has been shown that westerly winds at HKO are one of the favourable meteorological conditions for the occurrence of reduced visibility at that site. It was also found in the case studies that reduced visibility might occur during the onset of a weak northerly surge and on days with sea breezes. Lines of wind convergence could be observed in Hong Kong on such occasions. Winds were light on either side of the convergence line where high concentration of suspended particles could accumulate. These lines of convergence, while sweeping across Hong Kong, brought reduced visibility to the territory. Impairment in visibility was also observed during the approach of tropical cyclones from the east, probably related to the northwesterly winds brought to Hong Kong by their outer circulations and the stable atmosphere rendered by subsidence of air typically occurring ahead of tropical cyclones. In all cases, visibility dropped when winds abated but improved as winds strengthened.

Figure 12. Synoptic weather maps for 2 a.m. HKT on 16 and 17 August 1990.

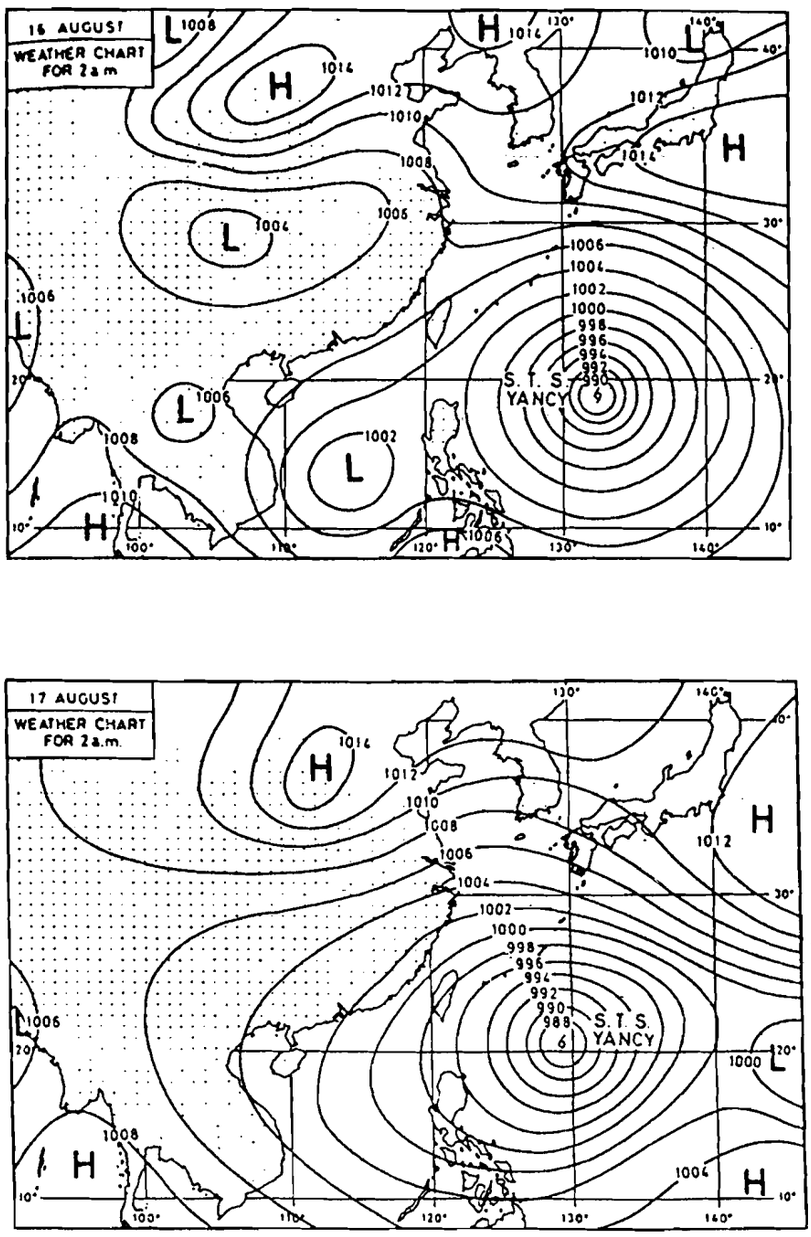

Figure 13. Wind flow over Hong Kong (a) at 8 p.m. HKT early on 16 August 1990, (b) at 6 a.m. HKT on 17 August 1990, (c) at 4 p.m. HKT on 17 August 1994 and (d) at midnight HKT late on 17 August 1990

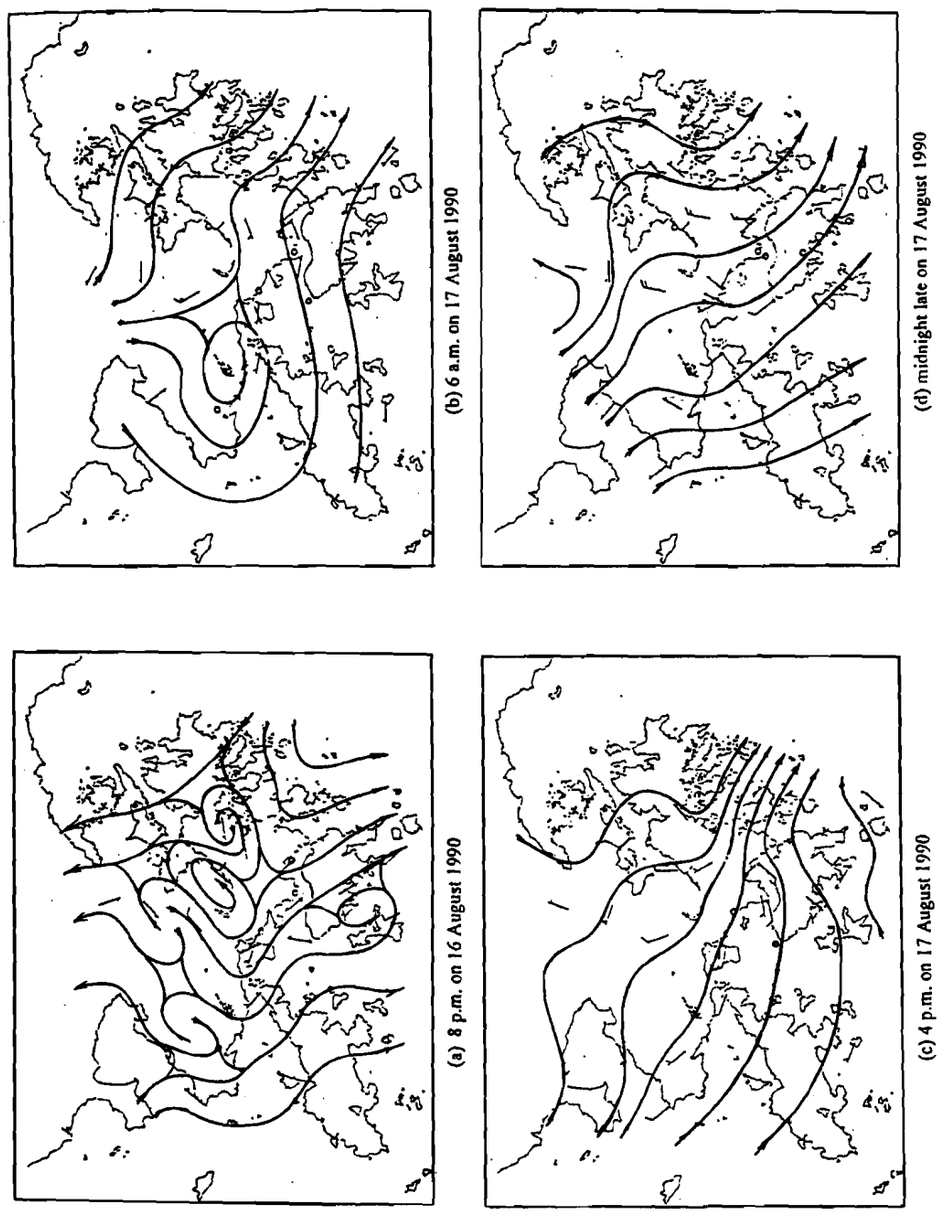

Figure 14. Wind at HKO, visibility at HKO and HKIA from 6 p.m. HKT on 17 August 1990 to 4 a.m. HKT on 18 August 1990

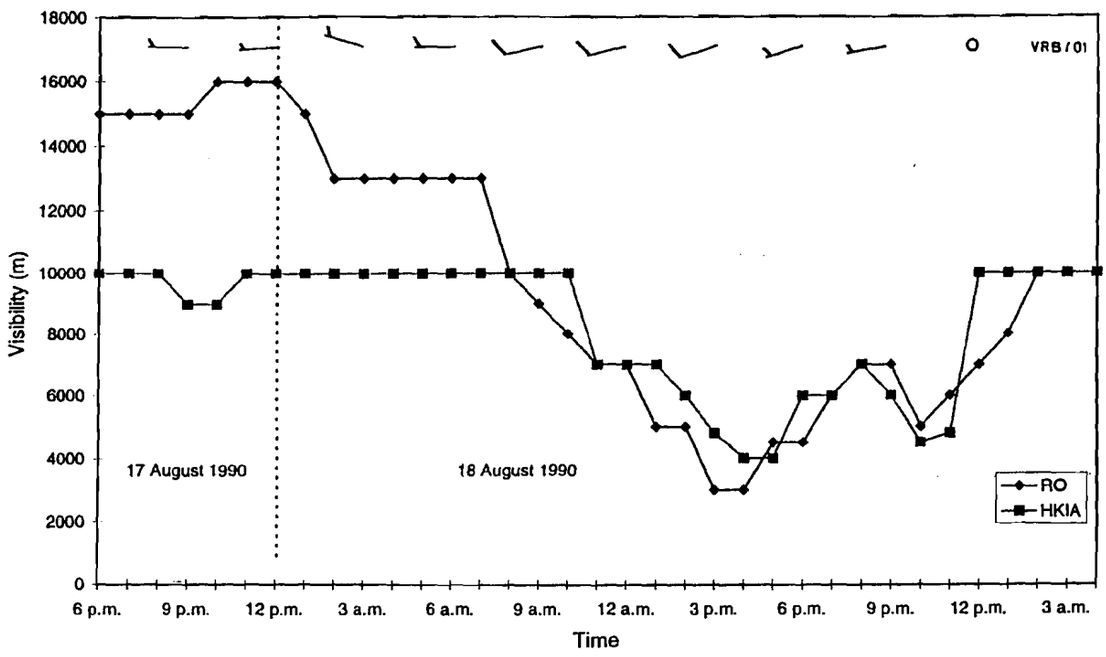

Acknowledgment

The authors would like to thank Mr. C.Y. Lam and Dr. W.L. Chang of the Hong Kong Observatory for their enlightening discussions and suggestions. Thanks should also be given to Mr. K.P. Wong and Mr. W.M. Chan for their assistance in preparing data for this study.

References

BELL G.J., P. PETERSON and P.C. CHIN, 1970: *Meteorological Aspects of Atmospheric Pollution in Hong Kong*, Royal Observatory Technical Note No. 29.

CHANG W.L. and E. KOO, 1986: A study of visibility trends in Hong Kong (1968-1982), *Atmospheric Environment*, 20, 1847-1858.

SLOANE C.S., 1982: Visibility trends - I. Methods of analysis, *Atmospheric Environment*, 16, 41-51.

Zhang, Lifeng and Zhang, Ming

LASG, Institute of Atmospheric Physics, Chinese Academy of Sciences, Beijing, China
and Department of Physics, The Chinese University of Hong Kong, Hong Kong

Study of the Sea-land Breeze System in Hong Kong

Abstract

The sea-land breeze system in Hong Kong is studied by using a modified Mass model for diagnosis. The effects of the large-scale background wind, localized urban heating and the differential solar heating of sun-facing mountain slopes are incorporated. The results are compared with an analysis of meteorological data over a ten-year period, and agree well with observations at Cheung Chau. The relatively fine grid of the numerical model (1 km × 1 km) allows spatial features to be resolved in a manner that would not have been possible using the observational data alone. The results from this study should be useful for weather forecasting, aviation safety and the understanding of the dispersal of air-borne pollutants in Hong Kong.

1. Introduction

Although Hong Kong has an area of only about 1000 km^2, its topography and physical features are complex. The main area is the New Territories and Kowloon Peninsula, with Hong Kong Island to the south and Lantau Island to the southwest, and over 200 islands in total. About 75% of the land area is hilly, and the highest peak rises to 957 m. The coastline and the mountains combine to give a terrain with many complex physical features (Figure 1).

As is well known, sea-land breezes are a kind of thermally induced local circulation found in coastal regions. They are driven by the differential heating rates over the sea and the land, and occur most visibly when the prevailing background wind is weak. Wai [1] has studied the secondary atmospheric circulation in Hong Kong. He extracted the secondary wind field at Waglan Island, and found that the wind direction has a clear diurnal variation which is found throughout the year but is especially significant in the winter months: the secondary wind field is northerly in the morning, and changes to southerly at about noon. This kind of secondary wind field associated with a diurnal reversal can be seen directly in daily observations as well. Figure 2 shows the wind data from meteorological stations in Hong Kong at 1400 LST, on 2 September 1996 and at 0200 LST, on 3 September 1996: the wind was basically northerly at 0200 LST and southerly at 1400 LST. It is clear that on this scale the stations are too sparse for the spatial structure of the wind system to be readily resolved.

Figure 1. Terrain map of Hong Kong area (grid resolution is 1 km).

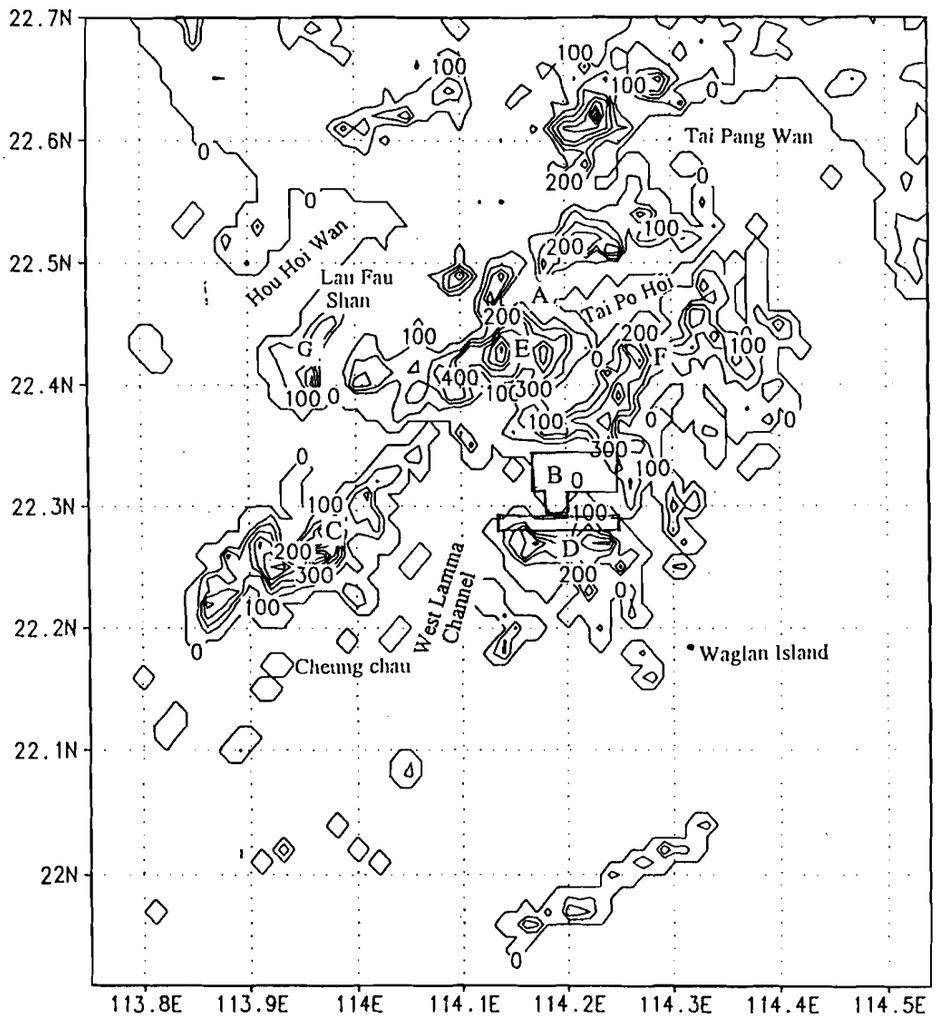

GrADS: COLA/UMCP

A. NEW TERRITORIES

B. KOWLOON

C. LANTAU ISLAND

D. HONG KONG

E. Tai Mo Shan

F. Ma On Shan

G. Castle Peak

Figure 2. Wind field recorded at meteorological stations in Hong Kong on 2 & 3 September, 1996: (a) 1400 LST 02; (b) 0200 LST 03.

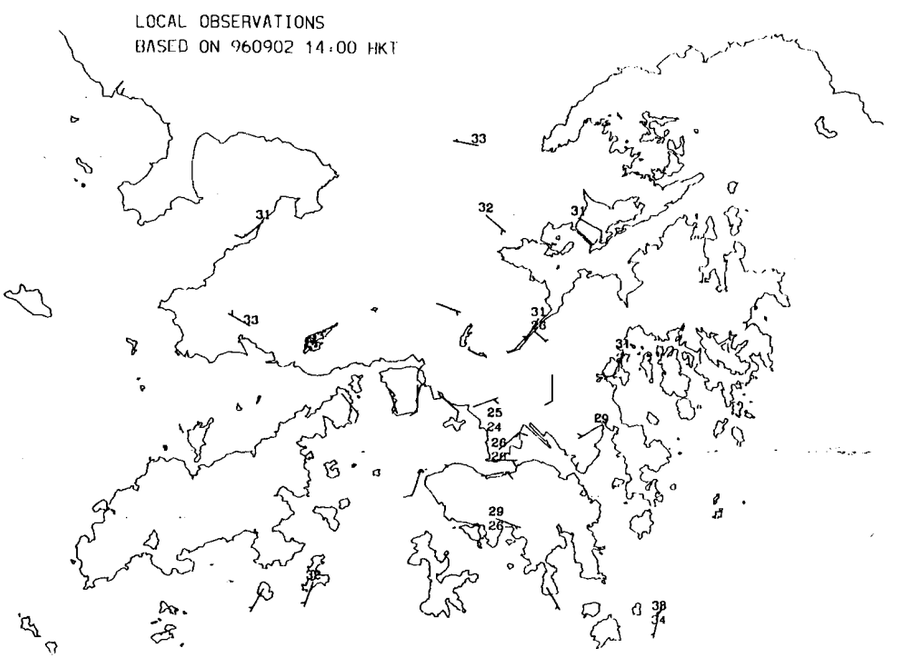

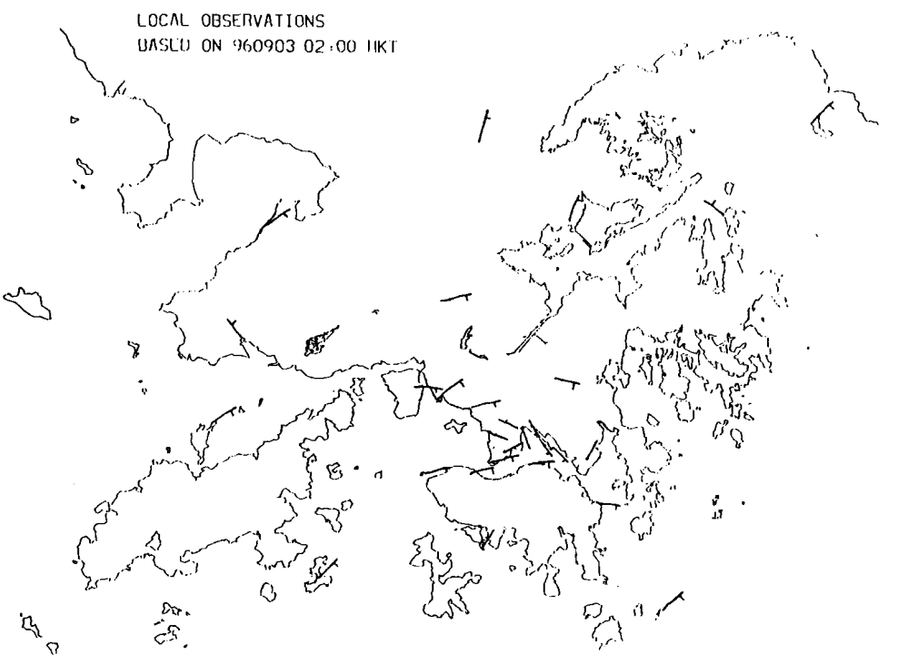

An interesting episode illustrates the importance of the variation of the wind direction with time and with local position --- both types of variation being important features of the sea-land breeze. On 2 February 1997, the first flight landed at the airport under construction at Chek Lap Kok. In that morning, an easterly background wind was observed in Hong Kong. Nevertheless, the duty aviation forecaster noted that at the scheduled time of landing later in the day, the sea breeze should have developed, and a local westerly wind was forecast for Chek Lap Kok [2]. The forecast turned out to be accurate, and the aircraft came in from the east-northeast, landing into the headwind.

Many studies about sea-land breezes have been carried out [3,4]. For example, Ohara [5] has studied the sea-land breeze over the Tokyo area. Zhong and Takle [6] have studied the sea-land breeze over the Kennedy Space Center-Cape Canaveral (KSC-CC) area. However, since the sea-land breeze is a mesoscale circulation, local characteristics are important. For Hong Kong, Chan and Ng [7] have suggested that the sea-land breeze has an important effect on the temperature recorded at coastal meteorological stations. Chan and Ng [8] have also studied the summer morning showers over Hong Kong, and have suggested that they are often caused by the convergence offshore between the land breeze at night and the prevailing large-scale monsoon flow. Clearly, the sea-land breeze influences weather in Hong Kong in significant ways.

An important question is the spatial structure of the wind systems associated with sea-land breezes in Hong Kong. Unfortunately, relatively little is known, despite the interest in this topic and its importance for local weather forecasting, aviation safety and studies of air pollution. This paper first analyses the meteorology data over a ten-year period (1980-1989) in order to capture the principal statistical characteristics of sea-land breezes over Hong Kong. However, the complicated structure of the coastline and of the terrain lead to a correspondingly complex spatial structure of the sea-land breeze wind system, with typical length scales of the order of ten km, which cannot be resolved by the station data alone. Therefore a fine-grid numerical model is developed for diagnosis, in order to infer the wind system between stations and to understand the mechanism in greater detail.

This paper reports on a statistical study of observational data and a diagnostic study using a modified mesoscale Mass model [9], which was developed precisely for the purpose of diagnosing surface winds in hilly and coastal regions. In order to resolve the fine spatial distribution of the sea-land breeze system in Hong Kong, the model resolution was chosen to be 1 km × 1 km (Figure 1). The results of the diagnostic study are found to agree reasonably well with the known observational data, and lead to insights about the sea-land breeze system for Hong Kong.

2. Observational Data

It is known that the wind direction at Cheung Chau station is heavily influenced by sea-land breezes. Figure 3 gives the diurnal wind direction recorded at Cheung Chau station, on 14, 15 and 16 September, 1995. On these three days, the sky was clear, and winds on the surface and at 850 hPa were influenced by a weak ridge of high pressure to the north. This kind of weather condition is favourable for the development of sea-land breezes. From Figure 3, it can be seen that Cheung Chau station experienced a variation of wind direction on each of these days: the wind was northerly in the morning, changed to southerly before noon, and changed back to northerly in the evening.

Figure 3. The diurnal change of wind direction at Cheung Chau, 14-16 September, 1995.

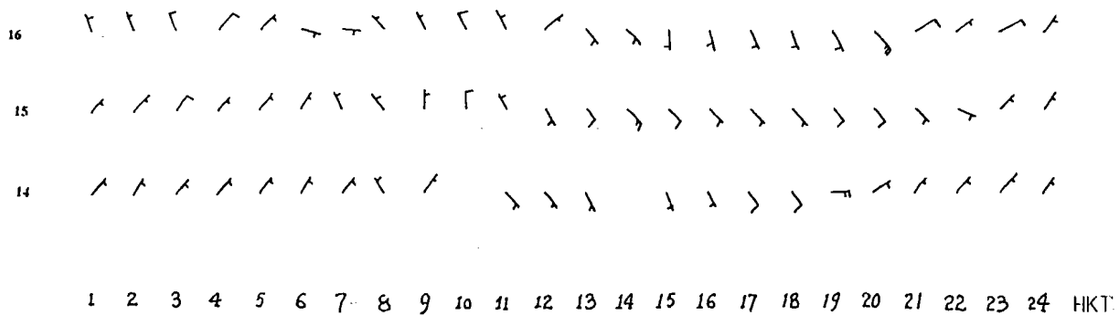

Given this prominent diurnal variation, we choose Cheung Chau as the index station for the occurrence of sea-land breezes in Hong Kong. A generally northerly wind (315° to 45°) at Cheung Chau is regarded as the land breeze and a generally southerly wind (135° to 225°) is regarded as the sea breeze. The occurrence of sea-land breeze is then defined by the observation of a change from northerly winds to southerly winds; this event marks the onset of the sea breeze while the subsequent change back to northerly winds signals the onset of the land breeze.

The meteorological data for Cheung Chau station over a ten-year period (1980-1989) were analyzed according to this definition (Table 1). Sea-land breezes occur on an average of 69 days per year, i.e., about one day in five. The most frequent occurrence was in 1980: sea-land breezes occurred one day in three. In general, the sea breeze typically onsets at about 1100 to 1200 LST, reaches a maximum speed of about 4 m s^{-1} three hours later, and lasts about nine hours. The monthly statistics, averaged over ten years, reveals a seasonal variation (Table 2). For example, the sea breeze lasts about 12 hours in the summer but only 8 hours in the winter. Sea-land breezes occur most frequently in December and January, and least frequently in June and July. The reason is that in the winter, Hong Kong is often influenced by the northeast monsoon and the sky is clear with no strong turbulence. This kind of weather is most favourable for the development of sea-land breezes. (While the summer months are often characterized by clear skies as well, the rypical southerly background would mask the sea breeze.) With weaker solar radiation in the winter, the onset of sea-land breezes is usually later, at about 1300 LST. In the summer, the strong solar radiation leads to an earlier onset of sea breezes; in July the sea breeze onsets at 1000 LST.

The data over ten years show that sea-land breezes are a significant feature of the local meteorology. However, the data and the statistical analysis refer only to Cheung Chau station, and the spatial structure of the wind system cannot be revealed by one station alone. In the absence of a sufficiently dense observational network, it is necessary to study the sea-land breeze system by a numerical diagnostic model with fine resolution.

Table 1. Statistics on sea-land breezes in Hong Kong, 1980-1989.

	1980	*1981*	*1982*	*1983*	*1984*	*1985*	*1986*	*1987*	*1988*	*1989*	*Mean*
Frequency of sea breeze (day)	104	69	80	52	64	57	91	53	35	81	69
Start of sea breeze (HKT)	11.0	11.8	11.7	12.1	12.4	11.8	11.7	12.3	11.8	11.4	11.7
Duration of sea breeze (hr)	8.0	8.5	10.9	8.8	6.8	9.2	10.5	7.2	10.1	9.9	9.0
Maximum sea breeze speed (ms^{-1})	4.7	3.7	3.5	4.0	3.8	4.1	4.6	4.0	4.2	4.6	4.1

Table 2. Monthly averages of the occurrence of sea-land breezes in Hong Kong.

	Jan	*Feb*	*Mar*	*Apr*	*May*	*Jun*	*Jul*	*Aug*	*Sep*	*Oct*	*Nov*	*Dec*	*Mean*
Frequency of sea breeze (day)	10	5	5	4	3	1	2	6	7	8	9	10	8
Start of sea breeze (HKT)	13	13	12	12	11	12	10	11	12	12	13	13	12
Duration of sea breeze(hr)	8	7	8	9	10	11	12	12	9	9	7	7	9

3. Diagnostic Model

This study uses the Mass model [9] to diagnose the sea-land breeze system in Hong Kong. The Mass model is a two-dimensional one-layer primitive model constructed upon the σ coordinate. It was formulated principally as a tool for the diagnosis of meso-scale phenomena involving complex terrain, and for the simulation of meso-scale phenomena such as sea-land breezes and valley winds under conditions when the large-scale background circulation is relatively steady. The model postulates a layer near the surface which is significantly influenced by the terrain. In addition, there is a reference layer through which the large scale initial field (geopotential height and temperature) are fed into the model. The temperature gradient between these two layers is given by the initial field, and is fixed throughout the simulation, but the temperature gradient within the surface layer depends dynamically on the surface temperature. Under these assumptions, and the hydrostatic approximation, the closed system of dynamic and thermodynamic equations on the surface ($\sigma = 1$) can be derived. For the present purpose, we chose a model resolution of 1 km, with 80 × 80 grid points (Figure 1). However, because we are concerned with lower latitudes and a relatively complex terrain, some modifications of the original Mass model are introduced.

(a) Initialization of the fields: The wind field over Hong Kong at 850 hPa (i.e., the reference level) is used for initialization. The potential height at 850 hPa for each grid point is calculated by the geostrophic relation. Then the surface wind is obtained by taking into account the vertical gradient of the wind field in the boundary layer, under the assumption that the pressure gradient force, the Coriolis force and the frictional force are balanced.

(b) Parameterization of drag coefficient: We assume that the surface drag coefficient C_d varies linearly with height, *i.e.*, $C_d = a Z_s + b$, where a and b are constants and Z_s is the terrain height. (Most works in the literature assume constant values of the surface drag coefficient; however, since the dependence on the terrain height is a key feature of the present model, it is appropriate to allow, through the simplest possible parameterization, a variation with height). The parameter values are $a = 0.08\ m^{-1}$, $b = 6.4 \times 10^{-4}$ over land, and $a = 0$, $b = 3.0 \times 10^{-3}$ over the sea.

(c) Forcing by the prevailing wind field: The prevailing background wind field can have a profound effect on the sea-land breeze. If the background wind is strong, the sea-land breeze may not occur; moderate background winds may interact with the sea-land breeze system to produce convergence either onshore or offshore, leading to precipitation in certain cases. So even though the sea-land breeze tends to occur when the background wind is weak, the latter must still be modeled. The background wind belongs to a much larger system, and in principle should be obtained from a larger model, allowing weather systems to advect into the domain under consideration. The background wind and the sea-land breeze on which it is superimposed will interact through the nonlinearities in the model equations, and in this sense the sea-land breeze is forced by the background. However, since the purpose of the present diagnostic study is not forecasting, it is convenient to model this forcing by separating out the sea-land breeze from the background prevailing wind, and dealing with the two components individually. Thus, the surface wind field $\vec{V}$ is separated into two parts in this study:

$$\vec{V} = \vec{U} + \vec{u} \tag{1}$$

Here, $\vec{U}$ is the prevailing surface wind, assumed to be a constant (in time and in space) in the model; $\vec{u}$ is the perturbation of the wind field due to the thermally forced sea-land breeze. At the start of the simulation, we set $\vec{u}$ to zero, and after a period of diabatic heating, the wind field $\vec{u}$ representing the sea-land breeze is generated, and evolves under the influence of the prevailing wind $\vec{U}$. Thus the momentum and heat transport equations take the form

$$\frac{\partial \vec{V}}{\partial t} = -\left(\vec{U} + \vec{u}\right)\nabla_\sigma \cdot \vec{u} - f\vec{k} \times \left(\vec{U} + \vec{u}\right) - \left(g\nabla_\sigma Z_s + RT_s\nabla_\sigma \ln p_s\right) + \vec{F} + K_M \nabla_\sigma^2 \vec{u} \tag{2}$$

$$\frac{\partial T_s}{\partial t} = -\left(\vec{U} + \vec{u}\right)\nabla_\sigma T_s + \frac{RT_s}{c_p}\left(\frac{\partial \ln p_s}{\partial t} + (\vec{U} + \vec{u}) \cdot \nabla_\sigma \ln p_s\right) + \frac{Q}{c_p} + K_T \nabla_H^2 T \tag{3}$$

where $\vec{k}$ is the unit vector in the vertical (upward) direction, T_s, p_s and Z_s are the surface temperature, surface pressure and surface height respectively, f is the Coriolis parameter, g is the gravitational acceleration, R is the gas constant, c_p is the heat capacity of dry air, K_M,

K_T are the horizontal momentum and temperature diffusion coefficients respectively, and $\vec{F}$ is the frictional force. The parameter values $K_T = K_M = 7 \times 10^3$ m^2 s^{-1} were adopted. (It is generally accepted that such effective parameters are grid-size dependent; the values chosen are adapted from the range in the original Mass model on account of the small grid size used in the present model.) The term $\nabla_H^2 T$ is the temperature diffusion at constant height rather than at constant σ. The normal diabatic heating rate is Q and the time dependence used in the model is shown in Figure 4. The diurnal variation is assumed to be sinusoidal, with a peak value at 1200 LST of Q_0 = 1 °C / hr on land and 0.25 °C / hr over the sea; the cooling is cut off to Q_1 = -0.25 Q_0 between 1800 LST and 0600 LST. The value of Q_0 compares with the values 0.75 °C / hr (land) and 0.17 °C / hr (sea) used in the literature for mid latitudes [9]. Changes from these normal values are explained below.

The perturbation field $\vec{u}$ is solved from Eq. 2 and Eq. 3, and the resultant wind field $\vec{V}$ is the sum of the background field $\vec{U}$ and the perturbation term $\vec{u}$. Because the equations are nonlinear, the two components interact in a nontrivial way.

Figure 4. The variation of diabatic heating rate with time.

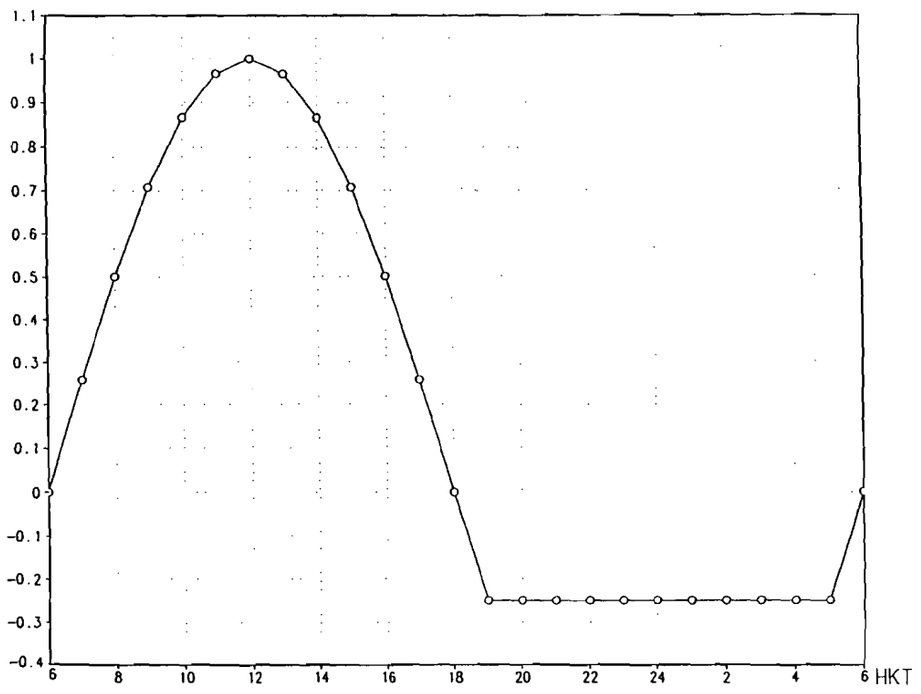

(d) Sun-facing slopes: As is well known, the different aspects of a mountain will receive different amounts of solar radiation, leading to different heating rates over the terrain. This effect is quite important for Hong Kong in view of its hilly terrain, and should be included in the model. For simplicity, the southern slope of any mountain is assumed to be sun-facing, and is assigned double the normal heating rate during the day; the opposite shaded slope is assigned the normal heating rate. The cooling rates at night are assumed to be identical.

(e) Urban heat pockets: Kowloon Peninsula and Hong Kong Island are developed urban areas, with tall buildings and a dense population, leading to fairly prominent urban heat pockets, not only in the daytime, but also at night; it is well known that the temperature in these urban areas is often higher than that in the surrounding areas [7]. Since the sea-land breeze is thermally forced, the urban heat pocket effect must be incorporated. In the present model, the areas of Kowloon Peninsula and Hong Kong Island (the central box in Figure 1) are assumed to be urban heat pockets; in the daytime, the heating rate is assumed to be double the normal value, while at night, the cooling rate is assumed to be 20% of the normal value.

4. Results and Analysis

First of all, the model was run without diabatic heating (i.e., setting $Q_0 = 0$); no sea-land breeze develops, showing that the sea-land breeze is driven by the diurnal diabatic heating. When diabatic heating is introduced, the sea breeze develops in the daytime and the land breeze develops at night.

The results are reported in three parts. First, we report results obtained with zero prevailing wind and without the sun-facing slope and the urban heat pocket effects (Section 4.1). Then the sun-facing slope and urban heat pockets are put in, and their effects are studied. The main branches of the sea-land breeze wind system and the associated convergence zones are discussed in detail (Section 4.2). Finally, the influence of various prevailing background winds is studied (Section 4.3).

4.1 Zero prevailing background wind

According to general observations, sea-land breezes occur most frequently when the prevailing background wind is very weak. It is therefore useful to first study the features of the sea-land breeze when there is zero prevailing background wind. In this subsection, we do not put in the sun-facing slope effect or the urban heat pockets.

Figure 5 gives the sea breeze at 1400 LST, and the land breeze at 0200 LST. The simulation shows that, at Cheung Chau station, the sea breeze is from the southwest (Figure 5a) and the land breeze is from the northeast (Figure 5b), in agreement with the observational data. The simulated wind directions at Lau Fau Shan and at Waglan Island also agree with the observational data. These verifications confirm that the basic features of the model are correct. We note that the sea breeze at Chek Lap Kok is westerly and the land breeze is easterly (Figure 5).

The wind system in the sea breeze is both stronger and more complex than that in the land breeze, and consists of three main branches: (a) westerly winds in the northern and the western parts of the territory, flowing inland from Hau Hoi Bay; (b) easterly winds in the eastern and

Figure 5. The distribution of the sea-land breeze under zero prevailing background wind when the sun-facing slope and the urban heat pocket effects are excluded.

(a) the distribution of the sea breeze.

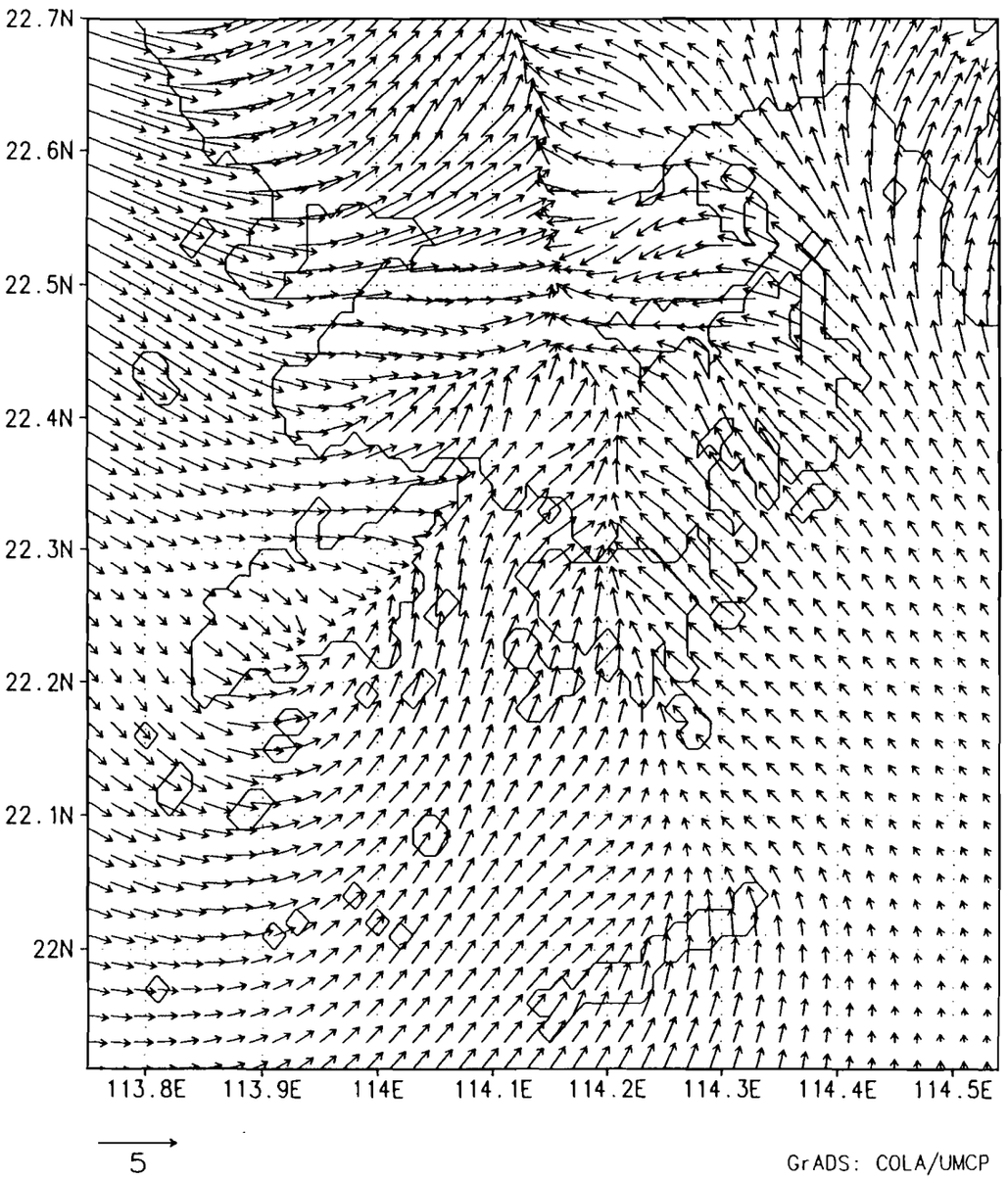

Figure 5 *(continued).*

(b) the distribution of the land breeze.

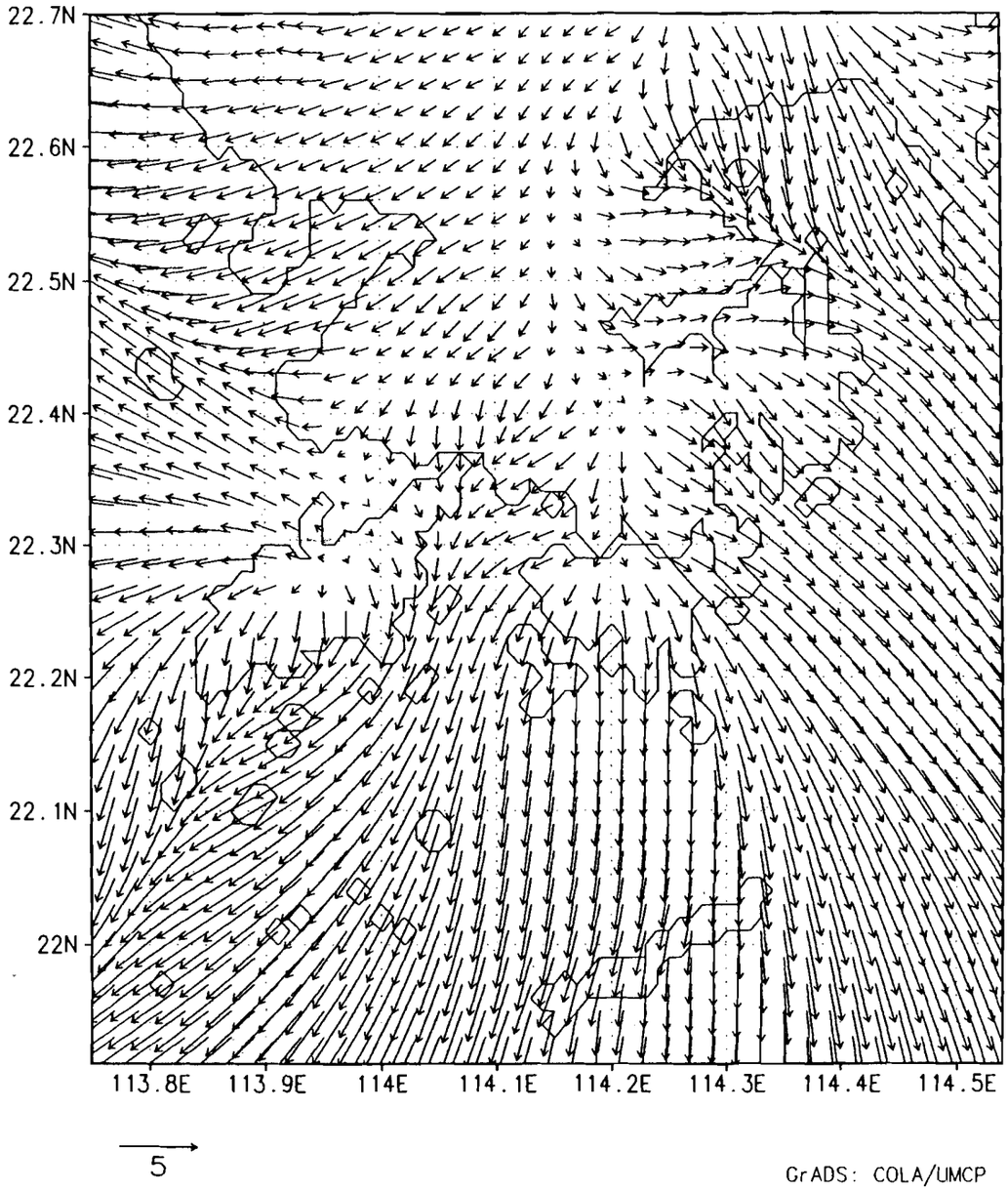

the northern regions, flowing inland from Tai Pang Bay; and (c) southerly winds to the south, which is especially prominent in the Lamma Channel, Hong Kong Island and over the sea to the southeast of Hong Kong Island.

The westerly and easterly branches meet in the central part of the New Territories, with fairly strong directional convergence between the two sides of the confluence zone. The westerly and the southerly branches develop two confluence lines in Lantau Island and from Castle Peak to Tai Mo Shan. The easterly and the southerly branches show a weaker confluence zone in the Ma On Shan area. In the southerly branch when the southeasterly sea breeze over the eastern part the Kowloon Peninsula meets the southwesterly sea breeze over the western part, a confluence zone is developed over Kowloon Peninsula and over Hong Kong Island.

We have also performed an experiment with the coastline only, but with all terrain removed (Figure 6). The three wind branches still exist, but the wind speed is weaker. The domain of each wind branch is also shifted. The influence of the terrain is the strongest on the southerly wind branch. The domain of the southerly wind is enlarged and the confluence in the southerly wind branch is weakened. When the terrain is removed, the easterly wind in the eastern part of the New Territories disappear, and instead a southeasterly wind appears.

These results from the diagnostic model demonstrate that the sea breeze wind system depends mainly on the contrast in the diabatic heating across the coastline. However the distribution and the domain of each wind branch and the confluence zones are related to the presence of the terrain which has not only a thermal but also a dynamic effect.

The land breeze phase is simpler in structure, and consists mainly of northerly winds over most of Hong Kong and a southeasterly wind over the northwestern part of Lantau Island (Figure 5b). There are still several confluence zones. The land areas on the two sides of Tai Pang Wan lead to one and another relatively weak zone is produced at Hau Hoi Wan due to the land breeze over the southwestern New Territories and the land breeze over the northwest of Lantau Island. There is also a confluence zone near the West Lamma Channel due to the land breeze over Lantau Island and over Hong Kong Island. It can be seen from Figure 5b that the northerly land breeze decreases in strength as it blows southwards over Kowloon Peninsula and Hong Kong Island, indicating another area of confluence.

4.2 The effect of sun-facing slopes and urban heat pockets

In order to obtain a more realistic picture of the wind system and the confluence zones, it is necessary to incorporate the sun-facing slope effect and the urban heat pocket effect. The clearest way to exhibit these effects is to analyse the divergence field.

For the sea breeze phase (1400 LST), Figure 7a shows the divergence field with neither the sun-facing slope effect nor the urban heat pocket effect, and Figure 7b shows the corresponding field when these two effects are incorporated. The wind branches and the convergence lines in the presence of the sun-facing slope and the urban heat pocket effects are seen more clearly in the conceptual model shown schematically in Figure 8. Three main features are worthy of note. (a) The three main branches remain qualitatively unaffected in their patterns. (b) The convergence at the south-facing slopes and at the point where the three wind branches meet are both strengthened, principally because of the sun-facing slope effect. (c) The convergence over Kowloon Peninsula and Hong Kong Island is enhanced in intensity and in extent, principally because of the urban heat pocket effect.

Figure 6. The distribution of the sea breeze systems for the case with coastline only.

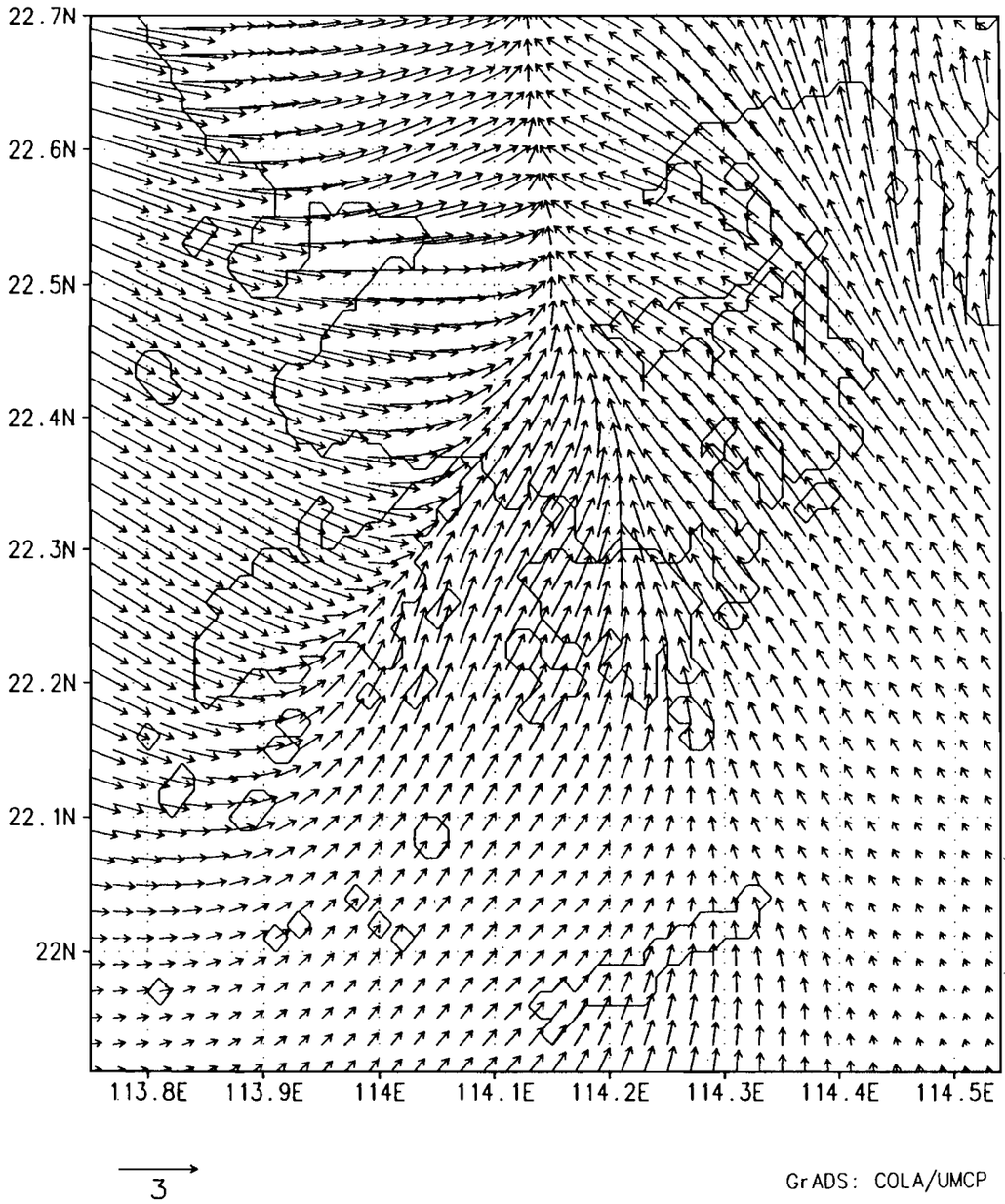

Figure 7. The divergence field for the sea breeze at 1400 LST.

(a) considering neither the sun-facing slope effect nor the urban heat pocket effect.

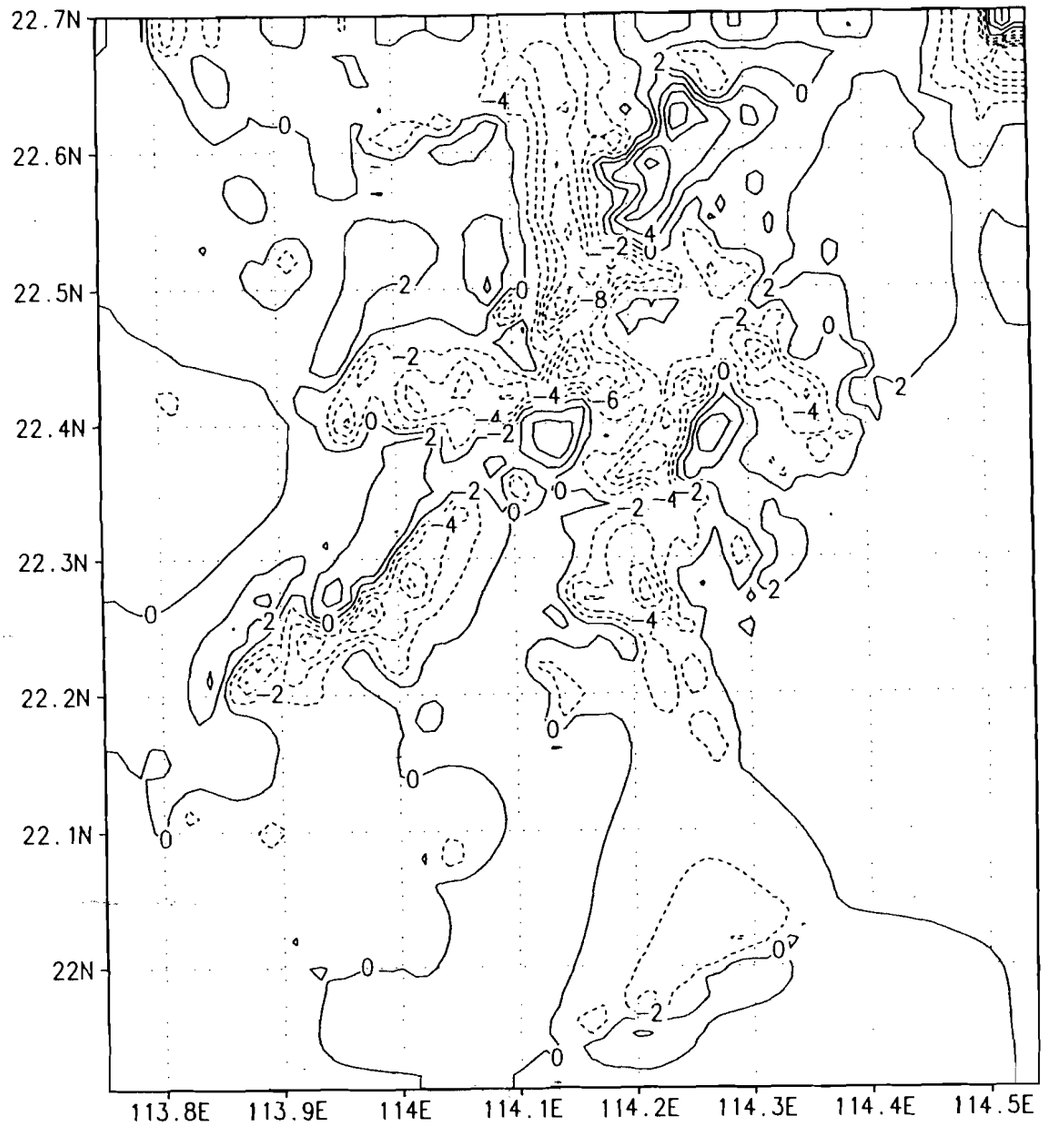

Figure 7 *(continued)*.

(b) considering both the sun-facing slope effect and the urban heat pocket effect.

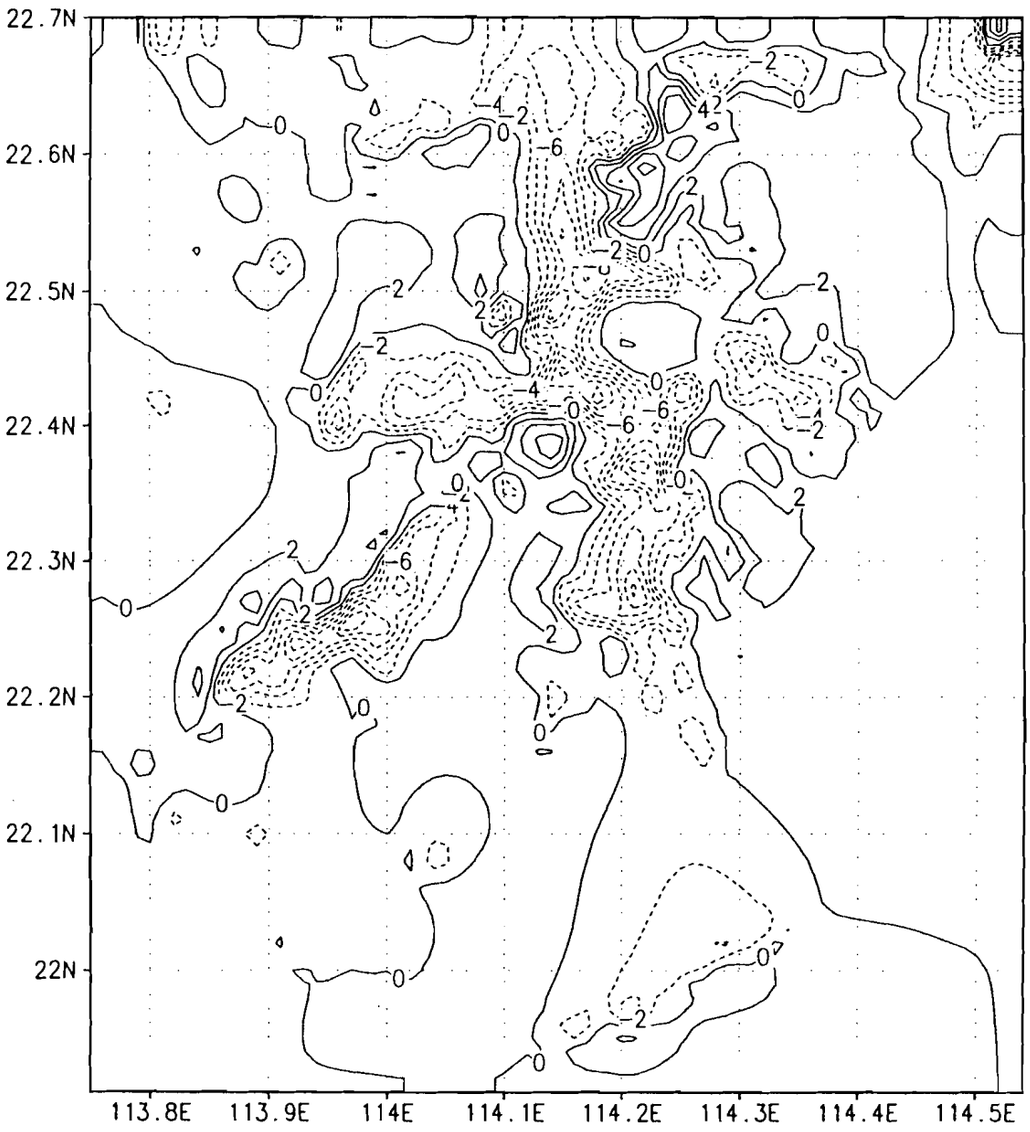

Figure 8. Schematic diagram showing the wind branches and the convergence lines in the sea breeze phase.

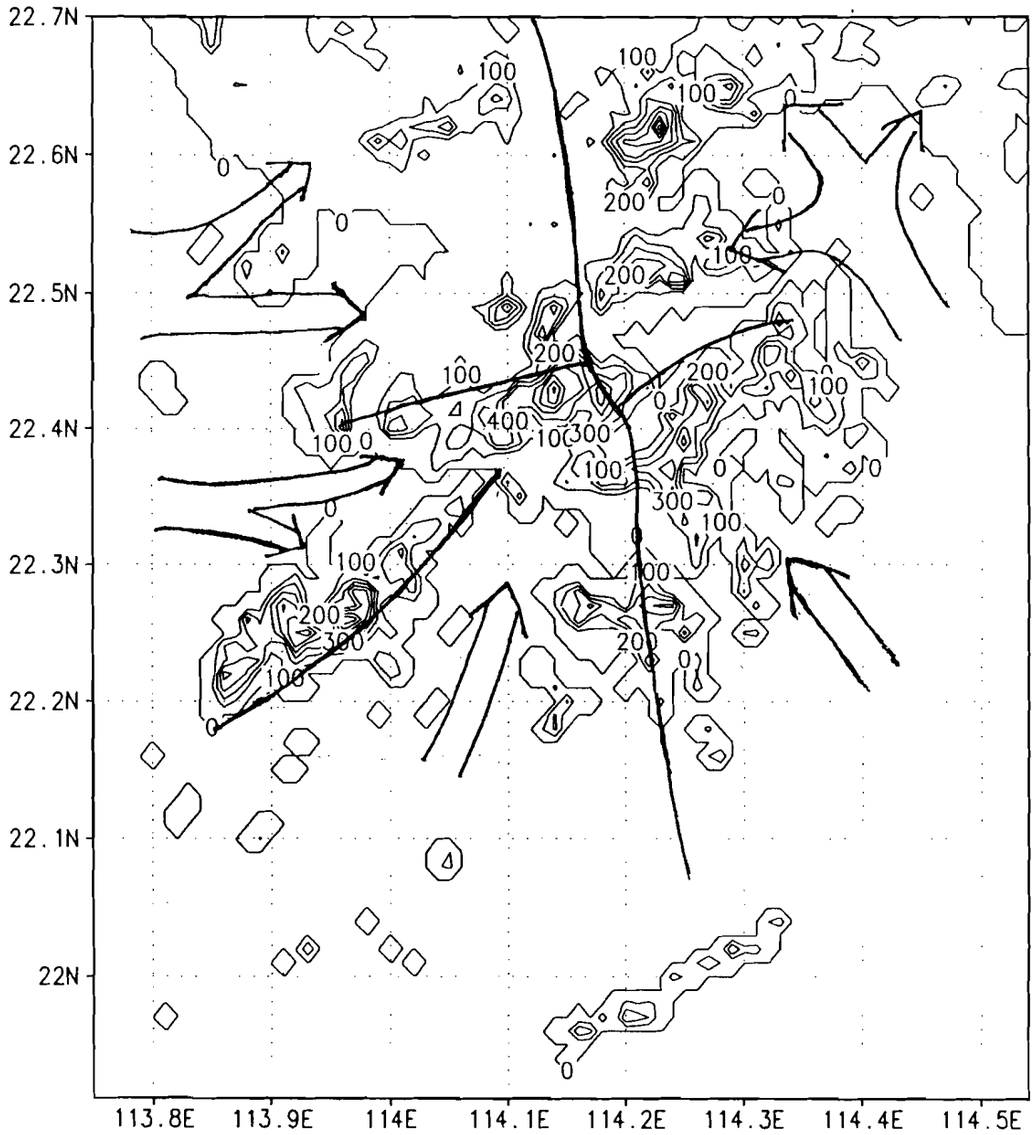

The relatively strong convergence over the urban areas can help to disperse air-borne pollutants when the vertical profile is unstable, but can also aggravate the local pollution when the vertical profile is stable. Moreover, the windshear associated with the convergence zones can have an effect on aircraft approaching to land (southbound) at Kai Tak International Airport, or on the flight path for take-off (northbound). However, the convergence line over Lantau is located inland, a distance from Chek Lap Kok, so that no major windshear is expected at the new airport as a result of the sea-land breeze. (It is of course a separate issue whether other weather systems can lead to windshear there.) In the land breeze phase (not shown), the convergence zone at the West Lamma Channel shifts to the east.

4.3 Prevailing background wind

When there is a prevailing wind, the distribution of the sea-land breeze wind system will be affected. A strong prevailing wind will mask the sea-land breeze, and we report below results obtained for a light prevailing wind of 2.0 m s^{-1} in the directions NE (typical of winter) and SW (typical of summer). The effect of urban heat pockets and sun-facing slopes are also included in the simulations.

The wind system consists of the three branches as mentioned before for any direction of the prevailing wind. However, the strength and coverage of each branch is slightly different. Usually, when the breeze is in the direction of prevailing wind, the strength of this wind branch is increased. Figure 9 gives the distribution of the sea breeze wind systems under the NE and SW prevailing winds. The most obvious difference occurs over Lantau Island and to the south. With a NE wind (Figure 9a), the convergence line over Lantau shifts inland towards the southwest, and the line is extended due south of Lantau. With a SW wind (Figure 9b) the convergence line over Lantau shifts slightly northwest (but still stays away from the coast and especially Chek Lap Kok), and the convergence line due south of Lantau disappears.

When the prevailing SW wind velocity is increased to 4 m s^{-1}, in the land breeze phase, a convergence line develops in the southern part of Hong Kong Island (Figure 10). This convergence is caused by the northerly land breeze and the SW prevailing wind, and may be related to summer morning showers over Hong Kong [8].

We have also performed other experiments with NW and SE prevailing winds (not shown). Compared with the distribution of the sea-land breeze under different directions of the prevailing wind, it is found that the sea breeze is the strongest with a NE prevailing wind. In the winter, Hong Kong is usually under the influence of a cold ridge of high pressure and a NE prevailing wind. When the prevailing NE wind is light, the sea-land breeze occurs frequently.

The effect of the prevailing background wind on the land breeze is somewhat simpler. In general, the land breeze is seen to be strengthened except when the background wind is northwesterly. The convergence zone at Hau Hoi Bay also shifts depending on the background wind. When the prevailing wind is easterly, the convergence is to the western part of the Lantau Island, but is not strong. When the prevailing wind is westerly, the convergence moves north and becomes strongest when the background is northwesterly.

Figure 9. The distribution of the sea breeze with the prevailing wind.

(a) the prevailing wind is northeasterly.

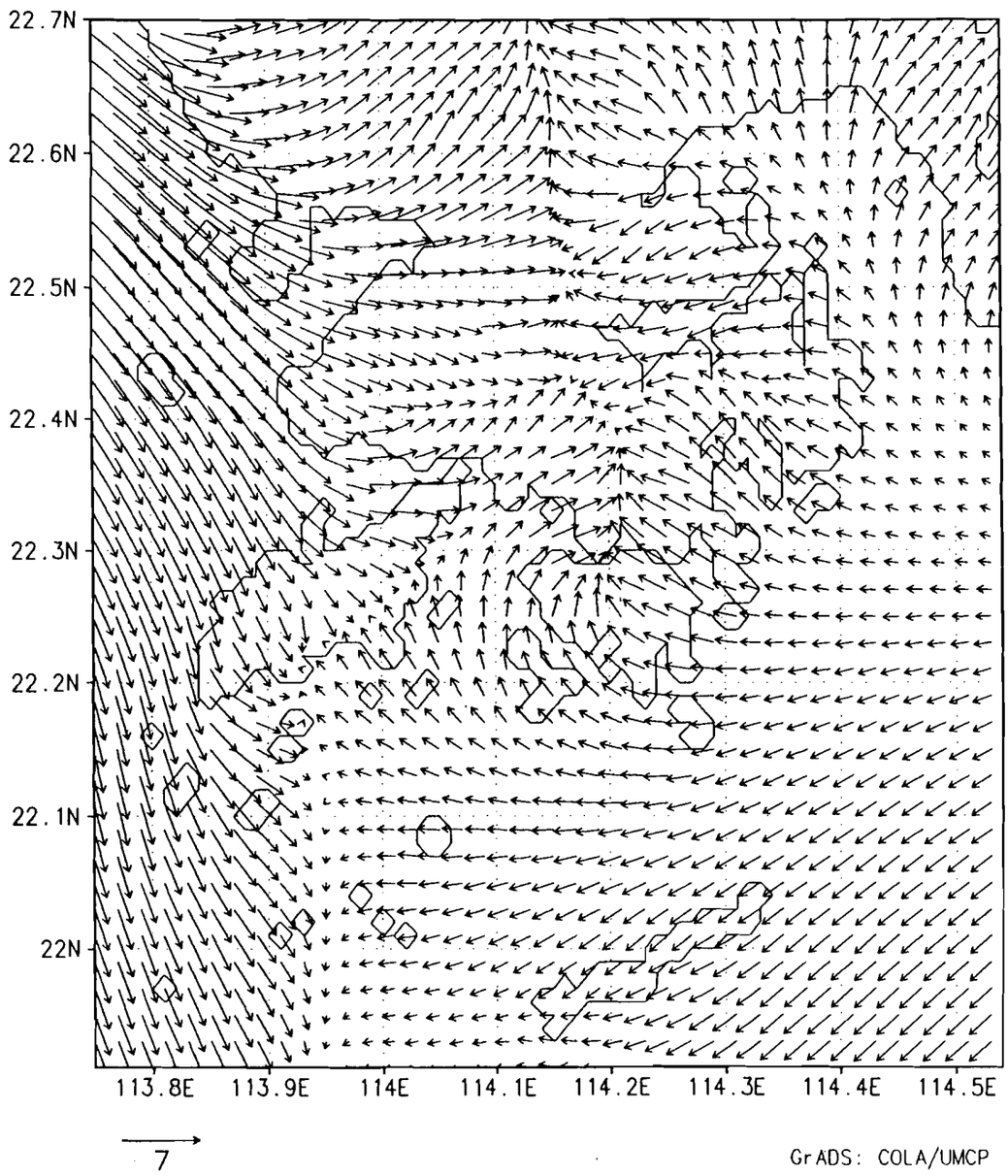

Figure 9 *(continued).*

(b) the prevailing wind is southwesterly.

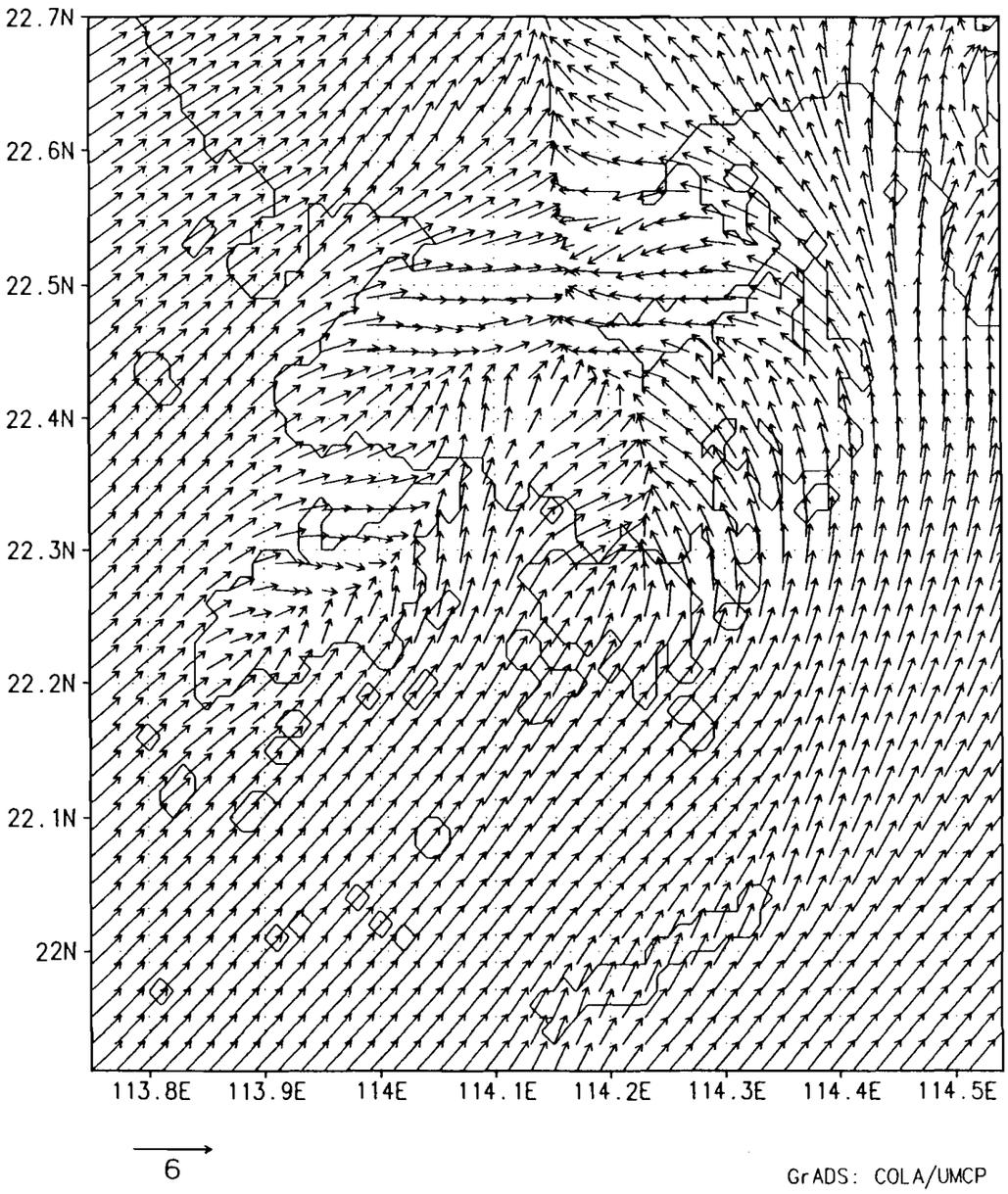

Figure 10. The distribution of land breeze with 4 m s^{-1} prevailing SW wind.

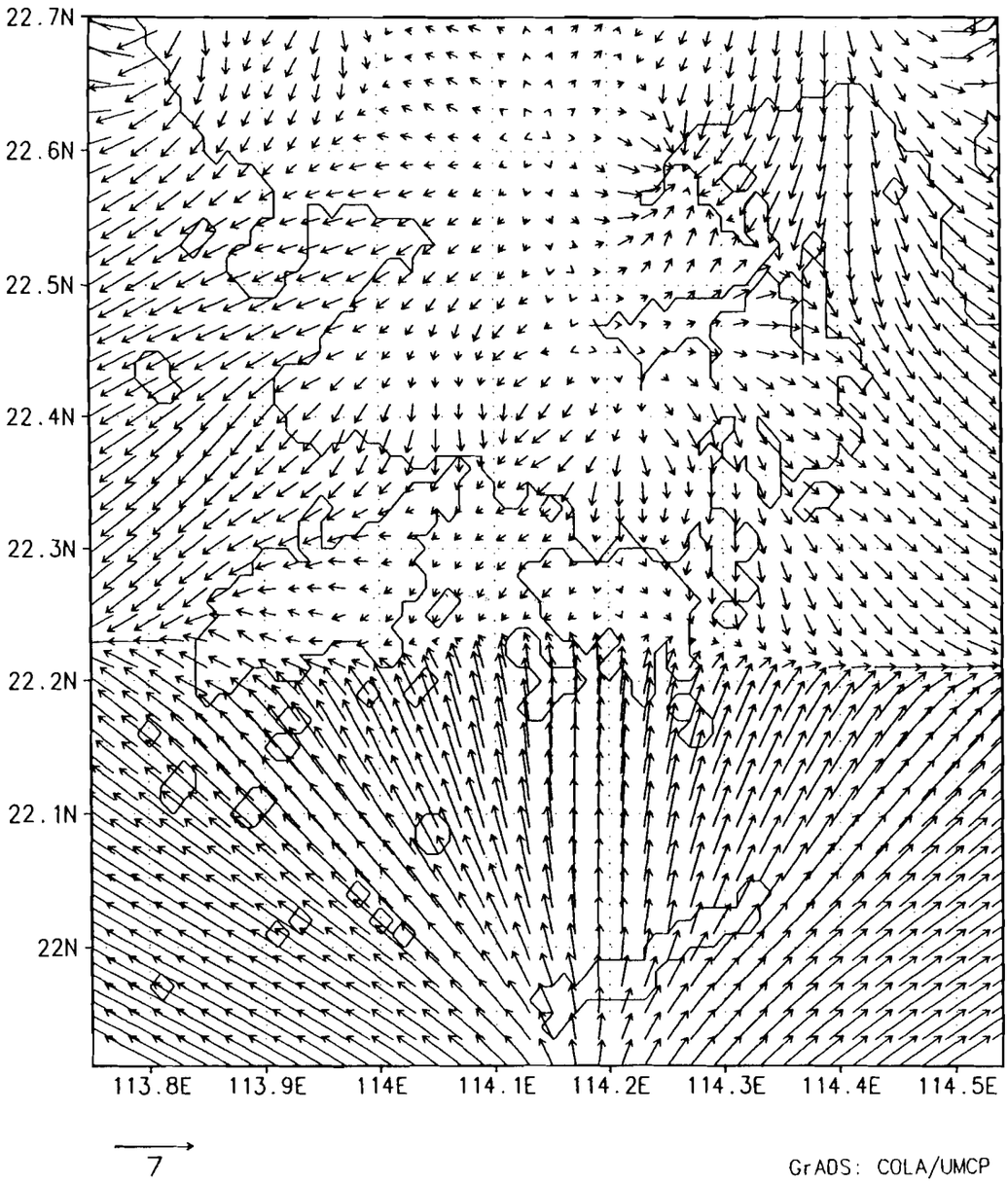

5. Conclusion

From the meteorological statistics and the diagnostic model, the following conclusions can be drawn.

(a) Hong Kong is often subject to the influence of sea-land breezes, with the highest frequency in the winter.

(b) A conceptual model of the sea-land breeze wind system has been developed from the diagnostic model. In the sea breeze phase, there are three wind branches, leading to various convergence zones. The land breeze wind system is somewhat simpler.

(c) The main features of the wind system are determined by the coastline, but the strength and the distribution of the three branches also depend on the terrain.

(d) Generally, the wind systems are only weakly modified by the sun-facing slope and urban heat pocket effects.

(e) The prevailing background wind modifies the strength and coverage of the three sea breeze branches.

Finally, the Mass model is a one-level model and cannot reveal the vertical structure of sea-land breeze. However, the parameters used in this study are climatic averages, *e.g.*, temperature gradient being 3.5×10^{-3} °C m^{-1}; the geopotential height of the reference layer (850 hPa) being 1511 m; and the temperature being 288 K. It may be better to use seasonal values, or even daily values in order to study variations throughout the year. However, since the sea-land breeze is driven by the diurnal cycle of differential heating, it depends mainly on the physical features of the coastline, which is already captured in this simple study.

6. Acknowledgements

We thank Prof. K. Young of The Chinese University of Hong Kong, Mr. C. Y. Lam and Mr. H. T. Poon of Hong Kong Observatory for their many helpful comments and suggestions. We also thank Mr. K. L. Lee and Mr. Y. C. Cheng of Hong Kong Observatory for the preparation of graphs and data. Mr. S. F. Ngan of The Chinese University of Hong Kong also assisted with some parts of the investigation. This work is supported in part by a grant from the Croucher Foundation.

References

[1] MAN-KUI WAI, MICKEY, 1993: Diurnal Atmospheric Secondary Circulations over Hong Kong, *HKMetS Bulletin*, 3 (2), 9-20.

[2] ANON, 1997: First landing at Chek Lap Kok, Newsletter of Friends of the Observatory, No. 3, April 1997.

[3] YEUNG, K.K., W.L. CHANG and B. WAN, 1991: Simulation of Boundary Layer Flow in Hong Kong, *Atmospheric Environment*, 25, 2161-2171.

[4] LOHAR, D., B. PAL and B. CHAKRAVARTY, 1994: Sea Breeze Activity at an Inland Station Kharagpur (INDIA) - A Case Study, *Boundary-Layer Meteorology*, 67, 427-434.

[5] OHARA T. and UNO I., 1989: Observed Structure of a Land Breeze Head in the Tokyo Metropolitan Area, *Journal of Applied Meteorology*, 28, 693-704.

[6] ZHONG S. and TAKLE, E., 1992: An Observation Study of Sea-land Breeze Circulation in an Area of Complex Coastal Heating, *Journal of Applied Meteorology*, 31, 1426-1438.

[7] CHAN, J.C.L. and T-K. NG, 1991: Temperature Variability over Hong Kong, *HKMetS Bulletin*, 1(2), 14-24.

[8] CHAN, J.C.L. and M H. NG, 1993: Morning Showers over Hong Kong During Summer, *HKMetS Bulletin*, 3(1), 14-24.

[9] MASS, C.F. and D.P. Dempsey, 1985: A One-level, Mesoscale Model for Diagnosing Surface Wind in Mountainous and Coastal Regions, *Monthly Weather Review*, 113, 1211-1227.

News and Announcements

This section is intended for dissemination of news and announcements by the Society or any of its members. If members wish to relay any news or make any announcement of interest to members which is related to the aims of the Society they should email, fax or mail such information to the Editor-in-Chief along with their name(s) and membership number(s).

UNEP's Environmental Effects of Ozone Depletion: 1994 Assessment available on-line at SEDAC

Date: Fri, 21 Feb 1997 13:57:44 -0500
Organization: University of Michigan

CIESIN and its Socioeconomic Data and Applications Center (SEDAC) are pleased to announce on-line availability of the United Nations Environment Programme's "Environmental Effects of Ozone Depletion: 1994 Assessment". The entire text of this document, regarded as the preeminent source of information regarding the impacts of increased ultraviolet radiation on the environment, is being provided for the first time through the SEDAC World Wide Web (WWW) site with permission from UNEP. The Uniform Resource Locator (URL)for the 1994 Assessment Table of Contents is:

http://sedac.ciesin.org/ozone/UNEP/UNEP94toc.html

The 1994 Assessment contains seven chapters:

(1) Changes in Ultraviolet Radiation Reaching the Earth's Surface
(2) Effects of Increased Solar Ultraviolet Radiation on Human Health
(3) Effects of Increased Solar Ultraviolet Radiation on Terrestrial Plants
(4) Effects of Increased Solar Ultraviolet Radiation on Aquatic Ecosystems
(5) Effects of Increased Solar Ultraviolet Radiation on Biogeochemical Cycles
(6) Effects of Increased Solar Ultraviolet Radiation on Tropospheric Composition and Air Quality
(7) Effects of Increased Solar Ultraviolet Radiation on Materials

The Introduction, Executive Summary, and three Appendices are also included.

In addition to the complete 1994 Assessment, UNEP's Environmental Effects of Ozone Depletion: 1996 Executive Summary report is also available through SEDAC's Stratospheric Ozone and Human Health Project home page. Links to both documents can be found in the "New" section of the Stratospheric Ozone and Human Health Project home page,

http://sedac.ciesin.org/ozone

For more information, please contact CIESIN User Services by e-mail at ciesin.info@ciesin.org or by telephone at 517/797-2727.

This service is provided by the Consortium for International Earth Science Information Network (CIESIN) under contract to the U.S. National Aeronautics and Space Administration (NASA) for the development and operation of the Socioeconomic Data and Applications Center (SEDAC). SEDAC is one of the data centers in NASA's Earth Observing System Data and Information System (EOSDIS). SEDAC's mission is to develop and deliver information products and services that integrate social and natural science data in ways useful for decision making.

CIESIN is a registered trademark of the Consortium for International Earth Science Information Network.

Free MTPE/EOS Data Products Handbook

Date: 02 March 1997

The Mission to Planet Earth/Earth Observing System (MTPE/EOS) Data Products Handbook provides high-level descriptions of the science and instrument data sets that will be produced from the Tropical Rainfall Measuring Mission (TRMM) and the first EOS satellite (AM-1). These data sets, which will provide essential information for science and policy research in the areas of global change and Earth system science, will be distributed to the user community through the EOS Data and Information System (EOSDIS). The document also contains information about the EOSDIS Distributed Active Archive Centers (DAACs) and the EOS instrument teams.

The 266-page document is available at no charge online or in hardcopy. The online version (in PDF format) is located at ftp://eospso.gsfc.nasa.gov/pub/sterling/DPH.pdf.

Hardcopy version are available from the Goddard Space Flight Center DAAC help desk:

Code 902 NASA GSFC Greenbelt, MD 20771 USA

Or call 301-614-5105 (M-F 8:30 am-4:30 pm), 1-800-257-6151,
or FAX 301-614-5268.

Please provide name, address, organization, phone number, and e-mail address.

Ozone investigation

Date: 13 March 1997
Organization: RdC

The "Universidad Tecnica Federico Santa Maria" in Chile (South America) is currently doing some investigation about the growth of the "ozone hole". If you are interested, here comes the project's home page:

http://ozono.dcsc.utfsm.cl

You have access to up to date graphics and animations taken from satellite photos and ground measurements from different points of our country.

Martin Stehr Santiago, Chile (South America) mstehr@rdc.cl

Joint International Symposium on Global Atmospheric Chemistry

Date: 13 March 1997

There is to be a Joint International Symposium on Global Atmospheric Chemistry (consisting of the 'Ninth Symposium of the IAMAS Commission on Atmospheric Chemistry and Global Pollution (CACGP) and the 'Fifth Scientific Conference of the International Global Atmospheric Chemistry Project (IGAC)'). A major theme is 'Atmospheric Chemistry and Climate Change'. The conference is on 19-25 August 1998 at Seattle in Washington state.

Email contact is: quinn@pmel.noaa.gov

Lee Grenfell, School of Chemistry, University of Birmingham,
Edgbaston, Birmingham B15 2TT, United Kingdom.
Tel. +44 (0121) 4145898 Fax. +44 (0121) 4143709

Global Soil Moisture Data Bank

Date: 16 March1997

Announcing the GLOBAL SOIL MOISTURE DATA BANK

http://metosrv2.umd.edu/~alan/soil_moisture/
Department of Meteorology University of Maryland

We are making available to the scientific community soil moisture observations from around the world. Currently we only have available 6 data sets from the former Soviet Union, but are in the process of preparing data sets for China, Mongolia, India, and Illinois. Please visit our site and send me comments and questions.

These data have been used for climatological analysis of soil moisture variations, land surface model validation and development, and ground truth (literally) for remote sensing of soil moisture, and we welcome you to use them for these and other purposes.

If you know of any other long-term actual observations of soil moisture or would like to contribute your data set, please also let me know. I can put in a link or provide an ftp site for downloading the data.

Prof. Alan Robock, Department of Meteorology
University of Maryland
College Park, MD 20742

Phone: (301) 405-5377
Fax: (301) 314-9482
Email: alan@atmos.umd.edu
http://www.meto.umd.edu/~alan

JPL Named A Partner In New Missions To Study Earth

Date: 18 March 1997
Organization: Jet Propulsion Laboratory

PUBLIC INFORMATION OFFICE
JET PROPULSION LABORATORY
CALIFORNIA INSTITUTE OF TECHNOLOGY
NATIONAL AERONAUTICS AND SPACE ADMINISTRATION
PASADENA, CALIF. 91109. TELEPHONE (818) 354-5011
http://www.jpl.nasa.gov

Contact: Mary A. Hardin

FOR IMMEDIATE RELEASE March 18, 1997

JPL NAMED A PARTNER IN NEW MISSIONS TO STUDY EARTH

Small, lower-cost spacecraft to study the distribution of Earth's forests and the variability of its gravity field have been competitively selected by NASA for development under a new Office of Mission to Planet Earth program, called Earth System Science Pathfinders (ESSP). NASA's Jet Propulsion Laboratory has been named a partner in the gravity mission and in an alternate atmospheric chemistry mission.

JPL will conduct the mission design and instrumentation on the Gravity Recovery and Climate Experiment (GRACE), led by Dr. Byron Tapley of the University of Texas at Austin. GRACE employs a satellite-to-satellite microwave tracking system between two spacecraft to measure the Earth's gravity field and its time variability over five years. Such measurements are directly coupled to long wavelength ocean circulation processes and to the transport of ocean heat to Earth's poles. GRACE includes major international cooperation with participation from Dr. C. Reigber, co-principal investigator from GeoForschungsZentrum (GFZ) in Potsdam, Germany.

JPL has also been selected as a partner in a proposed mission to better understand how atmospheric circulation controls the evolution of key trace gases, aerosols and pollutants over time. This mission was chosen as an alternate, should one of the primary missions encounter serious cost, scheduling or technical problems in its early development phases. Called the Chemistry and Circulation Occultation Spectroscopy Mission (CCOSM), this project would be led by Dr. Michael Prather of the University of California at Irvine.

The first mission to fly as part of the Earth System Science Pathfinders program is the Vegetation Canopy Lidar (VCL) mission, led by Dr. Ralph Dubayah of the University of

Maryland, College Park. The mission seeks to provide the first global inventory of the vertical structure of forests across Earth using a multibeam laser-ranging device. VCL will enable direct measurement of tree heights, forest canopy structures and derived parameters such as associate administrator for the Mission to Planet Earth program at NASA Headquarters, Washington, DC. "At the same time, they will cost-effectively complement NASA's Earth Observing System (EOS) program by addressing emerging research questions that will further expand our scientific knowledge of the Earth.

"Science value per dollar was the top criteria in this selection," Townsend added. "We also spent a great deal of effort validating the realism of the proposers' cost estimates and their technical readiness. For all of these reasons, the alternate mission should be considered a very real option should one of the selected missions unexpectedly encounter major difficulties."

"It also is important to note that the three selected missions collectively address all four major science research priorities of the U.S. Global Change Research program: land cover change, atmospheric chemistry, and both seasonal and long-term climate change," said Dr. Ghassem Asrar, Earth Observing System chief scientist at NASA Headquarters.

The ESSP selections were made from a group of 12 proposals that were evaluated in the second phase of a rigorous, two-phased selection process that began less than eight months ago with a July 1996 announcement of opportunity. This original announcement generated 44 proposals, which were initially reviewed for scientific merit. The review resulted in 12 proposals that met the requirements for the second phase of the ESSP evaluation.

As with NASA's Discovery program of small, focused space science-oriented spacecraft, the underlying philosophy of ESSP is to achieve maximum science value while complementing existing or planned flight missions. In the "principal investigator" (PI) mode for implementing ESSP, the single PI and his or her team are ultimately responsible for developing the flight mission hardware from selection to a launch-ready condition within 36 months, with minimal direct oversight from NASA. The PI and mission team are responsible for accomplishing the stated scientific objectives and delivering the proposed measurements to the broader Earth science community and general public as expediently as possible.

The laser mapping technique to be used by VCL, which was pioneered by NASA in aircraft experiments several years ago, should help resolve a major uncertainty in the scientific understanding of the global carbon cycle, particularly the role of terrestrial ecosystems in sequestering the atmospheric carbon dioxide produced by industrial activities and automobile exhausts. At the same time, the multibeam VCL lidar instrument will generate a vast array of reference points for future surveys of land topography, including the planned NASA-Department of Defense Shuttle Radar Topography Mission in 1999-2000. VCL measurements should also have practical commercial applications in forestry management.

The total mission life-cycle cost to NASA of VCL is $59.8 million, including the launch vehicle. VCL will be launched in spring 2000 on a Pegasus launch vehicle. Industrial partners in VCL include CTA Space Systems, McLean,VA; Fibertek Inc., Herndon, VA; and Omitron Inc., Greenbelt, MD, with participation by scientists at NASA's Goddard Space Flight Center, Greenbelt, MD, and several U.S. universities.

GRACE will provide a framework for studying the gravitational signatures of gigantic, continent-sized underground water reservoirs, or aquifers. It also will provide a never-before-available

perspective on global ocean circulation and the time variability of Earth's overall external shape, or geoid. This fundamental data set could enable great improvements in existing ocean radar altimetry data sets, and retrospective improvements of seasonal to inter-annual climate change estimates.

Through an innovative teaming arrangement, GRACE's German partner, GFZ, will provide mission operations and a Russian booster for a spring 2001 launch, greatly reducing the direct total cost to NASA, which is $85.9 million. In addition to JPL, other partners include Loral Space Systems, Palo Alto, CA, and Dornier of Germany to build the spacecraft.

The Chemistry and Circulation Occultation Spectroscopy Mission would make at least 18 months of measurements of the vertical distribution of more than 30 diagnostic trace gases and aerosol properties. Such data will provide never-before-available chemical and physical boundary conditions from which to model the behavior of the chemistry of Earth's atmosphere, such as the mixing of pollutants in the lower atmosphere. Measurements to be acquired by CCOSM will be used in conjunction with general atmospheric circulation models to assess the effectiveness of the Montreal Protocol (i.e., the banning of chlorofluorocarbons and other potentially harmful gases) on controlling the depletion of atmospheric ozone.

In addition to JPL, partners in CCOSM include Lockheed-Martin Infrared Imaging Systems, Lexington, MA, and Spectrum Astro Inc., Gilbert, AZ.

In addition to the funding support for the science team associated with each mission, NASA has set aside 10 percent of the annual budget for the ESSP program to support innovative use and analysis of the observations resulting from the ESSP missions. The intent is to utilize these funds to support science data analysis and research investigations through an open solicitation and peer review process once data from the ESSP missions become available. NASA intends to solicit another set of ESSP missions in the fall of 1998.

The ESSP program is a new element of NASA's Office of Mission to Planet Earth, a long-term, coordinated research enterprise designed to study the Earth as a global environmental system.

Heat Wave Deaths Projected to Increase in Cities

Date: 01 April 1997

Over the next 25 years, the number of deaths resulting from hot weather is expected to rise significantly in many of the 44 largest metropolitan areas in the United States, according a new study by Laurence Kalkstein of the University of Delaware Center for Climate Research.

During the summer heat wave of 1995 in Chicago, the severe impact of extreme temperatures on human health was illustrated by the tragic deaths of more than 700 people. Such events are likely to become far more common over the next 60 years, Kalkstein said, with death tolls increasing by as much as two-fold by 2050.

These figures remain possible, despite allowances in the research for people to grow more accustomed to warmer temperatures, the study notes.

The study also points out that extreme heat does not "only" kill people who are already on the verge of death. While many people believe that those killed by a heat wave would soon have died anyway because of other causes, Kalkstein said this "mortality displacement" effect currently accounts for only 40 percent of excess mortality in most areas.

Under the most conservative of three climate change scenarios used in the study, the moist tropical air masses in New York City that prove most deadly in the summertime are expected to double in frequency by 2020. This could drive heat wave deaths up by 18 percent, the study says. The other scenarios in the study yield up to six-fold increases in high-risk weather days -- resulting in a mortality ranging from 62 percent to 145 percent.

"Similar magnitude increases in summer high-risk air masses are noted for virtually all of the large Midwestern and eastern cities where weather/mortality relationships are strong," reported Kalkstein.

Because winter mortality rates have more to do with respiratory and other diseases unrelated to daily air mass conditions, the study's projection show relatively little decrease in winter death rates as a result of climate change.

Contact: Environmental Media Services, phone 202-463-6670.

Low Ozone Measured Over North Pole

Date: 8 April 1997
Organization: Jet Propulsion Laboratory

Donald Savage
Headquarters, Washington, DC
(Phone: 202/358-1547)

Allen Kenitzer
Goddard Space Flight Center, Greenbelt, MD
(Phone: 301/286-2806)

Barbara McGehan
National Oceanic and Atmospheric Administration, Boulder, CO
(Phone: 303/497-6288)

RELEASE: 97-64 8 April 1997

LOW OZONE MEASURED OVER NORTH POLE

Unusually low levels of ozone over the Arctic were measured during March by satellite-based monitoring instruments operated by NASA and the National Oceanic and Atmospheric Administration (NOAA).

"These are the lowest ozone values ever measured by the TOMS instruments during late-March and early-April in the Arctic," said TOMS Project Scientist, Dr. Pawan K. Bhartia, of NASA's Goddard Space Flight Center (GSFC), Greenbelt, MD. "However, these low ozone amounts are still nearly a factor of two greater than the lowest values seen by TOMS in the Antarctic during Southern hemisphere Spring."

Centered in a stable, nearly circular region over the North Pole, the average March 1997 ozone amounts were 40 percent lower than the average March amounts observed between

1979 and 1982. This follows ozone amounts in March 1996 that were 24 percent lower than the 1979-82 average, although this low was off center of Earth's pole toward the North Atlantic.

The minimum in total column ozone fell to 219 Dobson units on March 24, 1997, from values near 280 units earlier in March. Two NASA Total Ozone Mapping Spectrometer (TOMS) instruments, one aboard NASA's Earth Probe (TOMS-EP) satellite and the other aboard Japan's Advanced Earth Observing Satellite (ADEOS) made the measurements of the rapid decrease, supported by similar data from the Solar Backscatter Ultraviolet instruments aboard the NOAA-9 and NOAA-14 satellites.

The Halogen Occultation Experiment (HALOE) aboard NASA's Upper Atmosphere Research Satellite (UARS) measured vertical distributions of ozone that confirm these low Arctic values. On March 26, HALOE measured a very low ozone concentration of less than one part per million of ozone (normal concentrations are near 3-4 parts per million) at an altitude of 12.4 miles slightly northeast of Hudson's Bay.

Over the Alaskan Arctic, where NOAA monitors ozone from the surface at Barrow, Alaska, March average ozone was about 375 Dobson units, slightly below the March average for the past ten years of 413 Dobson units, according to David Hofmann, Director of NOAA's Climate Monitoring and Diagnostics Laboratory in Boulder, CO. "On March 17 and 18 ozone dipped to values below the 300 Dobson unit range when the edge of the low ozone region extended to the latitude of Barrow (71 degrees north)," he said. "This is not a typical occurrence and indicates the unusual conditions this year."

"The unusual meteorological conditions played a significant role in the March ozone lows," according to Paul A. Newman of the GSFC. "The reason or reasons behind these unusual stratospheric weather patterns are unclear, and figuring out why this pattern occurred will be a significant component of our further research efforts."

Furthermore, measurements from balloon-based ozone instruments operated by Environment Canada and launched from Eureka (80 degrees North latitude) and Resolute Bay (75 degrees North) reveal 60 percent ozone losses between the altitudes of 6.2-15.5 miles during March, in comparison to historical March observations.

The TOMS data show that the region of low ozone amounts below 280 DU exceeded 5.3 million square kilometers, covering a substantial fraction of the Arctic region. These low ozone amounts are found inside the Arctic polar vortex, a part of the stratospheric circumpolar jet stream.

The 1996/1997 winter polar vortex has been unusually strong and persistent into March. Data from NOAA's Climate Prediction Center show cold temperatures low enough to form polar stratospheric clouds during late March. These clouds, common in January and February but rare in late March, helped convert certain forms of stratospheric chlorine into forms which are highly reactive to ozone destruction. The combination of reactive chlorine compounds and sunlight from the March rising sun at polar latitudes leads to destruction of ozone.

The most recent observations indicate that temperatures had become too warm by March 30 for polar stratospheric clouds to form. In addition, the minimum ozone amounts in the Arctic have begun to slowly increase from the unusually low March amounts, and the area covered by

the low has begun to decrease.

"The appearance of this well-defined region of low ozone is consistent with our expectations following detailed chemical analyses of the Arctic winter stratosphere in early 1989 and 1992," said Dr. Michael Kurylo, manager of NASA's Upper Atmosphere Research Program, which organized those airborne experiments. "The persistence of such cold temperatures within the Arctic vortex well into the sunlit period is an essential ingredient for driving many of the chemical cycles for ozone destruction. We will now be examining these low ozone air masses into their recovery period using our best satellite and airborne instruments."

An international treaty on ozone-depleting substances is leading to reductions in their concentrations in the atmosphere and hence to reduced chlorine levels in the stratosphere. As we move into the next century, chlorine-catalyzed ozone losses resulting from CFCs and other chlorine-containing species will be reduced.

Ozone, a molecule made up of three atoms of oxygen, absorbs harmful ultraviolet radiation from the Sun. Most atmospheric ozone is found in a thin layer between 6-18 miles. A Dobson unit is related to the physical thickness of the ozone layer if it could be brought down to the Earth's surface. The global average ozone layer thickness is 300 Dobson units, which equals 1/8th of an inch, approximately the thickness of two stacked pennies. In contrast, the ozone layer thickness in the Antarctic ozone hole is about 100 Dobson units (1/25th of an inch), approximately the thickness of a single dime.

TOMS ozone data and pictures from March 1997 are available on the Internet at the following URL: http://jwocky.gsfc.nasa.gov or through links on: http://pao.gsfc.nasa.gov/

TOMS-EP, ADEOS, and UARS, and the aircraft, balloons and ground-based ozone-measurement programs are key parts of a global environmental effort which includes NASA's Mission to Planet Earth, a long-term, coordinated research effort to study the Earth as a global environmental system.

The TOMS instruments are managed by Goddard. The HALOE instrument is managed by NASA's Langley Research Center, Hampton, VA. NOAA-9 and NOAA-14 are managed by the NOAA National Environmental Satellite, Data, and Information Service, Suitland, MD.

Higher Education Global Change Courses

Date: 21 April 1997

The US Global Change Research Information Office (GCRIO) is putting together a web page of global change courses in higher education and is looking for suggestions.

The page currently lists 42 courses at 30 universities and is located at:

http://www.gcrio.org/edu/highered.html

The links on the page range from simple course descriptions to course home pages. The primary focus is on interdisciplinary/integrative courses.

If you have a course that you would like us to consider adding to the list, or one that you prefer to have removed, please let me know. The GCRIO is especially interested in adding global change courses from non-US institutions.

Joe Schumacher, U.S. Global Change Research Information Office
2250 Pierce Rd., University Center MI 48710
Ph: 517-797-2730 Fx: 517-797-2622 http://www.gcrio.org

New Data Available from LaRC DAAC

Date: 21 April 1997

EOSDIS RADIATION BUDGET, CLOUDS, AEROSOLS and
TROPOSPHERIC CHEMISTRY DATA

Langley Distributed Active Archive (Langley DAAC)

WWW: http://eosdis.larc.nasa.gov/
e-mail: larc@eos.nasa.gov

The Earth Observing System Data Information System (EOSDIS) Langley Research Center Distributed Active Archive Center (DAAC) announces the release of the Global Tropospheric Experiment Pacific Exploratory Mission in the Tropical Pacific (GTE PEM Tropics) data. The initial availability of this data is through the Langley DAAC Home Page at http://eosdis.larc.nasa.gov/. This new data as well as all of the GTE data currently archived at the Langley DAAC are now available for direct download from the Langley DAAC home page. Follow the "Access Data" link then the "Data Accessible from the Web" link. Follow the "Download Data" link and register to gain access to the GTE data. Note for convenience the data files have been "zipped" to facilitate transfer.

THESE DATA PRODUCTS ARE FREE OF CHARGE.

TYPES OF DATA:
The Langley Distributed Active Archive Center, located in Hampton, Virginia, is responsible for the archival and distribution of NASA science data in the areas of radiation budget, clouds, aerosols and tropospheric chemistry. The Langley DAAC will also archive some of the data sets which result from the EOS program and other elements of Mission to Planet Earth. Currently archived and available for distribution is data from the Earth's Radiation Budget Experiment (ERBE); the International Satellite Cloud Climatology Project (ISCCP); the Stratospheric Aerosol and Gas Experiment (SAGE) ; the Surface Radiation Budget (SRB); the First ISCCP Regional Experiment (FIRE); the Global Tropospheric Experiment (GTE); the Stratospheric Aerosol Measurement (SAM) II; the Aerosol Research Branch (ARB); Measurement of Air Pollution from Satellites (MAPS); Biomass Burning; NASA Water Vapor Project (NVAP); Nimbus 7 ERB; Scanning Multichannel Microwave Radiometer (SMMR); Smoke/Sulfates, Clouds and Radiation (SCAR) and Subsonic aircraft: Contrail & Clouds Effects Special Study (SUCCESS).

HOW TO CONTACT US

For information regarding Langley DAAC data or to place an order, please contact:

Langley DAAC Science, User and Data Support Office
NASA Langley Research Center, Mail Stop 157D
Hampton, VA 23681-0001

Phone: (757) 864-8656 Fax: (757) 864-8807 Internet: larc@eos.nasa.gov

New SAGE II CD-ROM from LaRC DAAC

Date: 21 April 1997

EOSDIS RADIATION BUDGET, CLOUDS, AEROSOLS and TROPOSPHERIC CHEMISTRY DATA

Langley Distributed Active Archive (Langley DAAC)

WWW: http://eosdis.larc.nasa.gov/ e-mail: larc@eos.nasa.gov

The Langley Distributed Active Archive announces the availability of the Stratospheric Aerosol and Gas Experiment II (SAGE II) CD-ROM. The CD-ROM is ISO9660 compliant allowing PCs, Macintoshes and Unix machines all to access it. The CD-ROM contains SAGE II monthly mean global color image maps and the relevant gridded data for aerosol extinction at 1020 nm, 525 nm, 453 nm and 385 nm wavelength, ozone mixing ratio, water vapor mixing ratio and relative humidity, nitrogen dioxide mixing ratio at up 14 pressure levels. By providing the SAGE II monthly mean color maps and gridded data, the SAGE II data will be easily accessible to a larger community. The visual maps provide for a quick scan of the monthly retrievals, while the gridded data should be helpful for analysis and can be used as input for othergraphical presentations and statistics.

This CD-ROM may be ordered from the Langley Distributed Active Archive (Langley DAAC) home page at http://eosdis.larc.nasa.gov/ by following the "Access Data" link to the Order Form for CD-ROMs and Videocassettes. More information may be obtained from the Langley DAAC Science, User and Data Services Office at larc@eos.nasa.gov.

THIS DATA PRODUCTS IS FREE OF CHARGE.

TYPES OF DATA:
The Langley Distributed Active Archive Center, located in Hampton, Virginia, is responsible for the archival and distribution of NASA science data in the areas of radiation budget, clouds, aerosols and tropospheric chemistry. The Langley DAAC will also archive some of the data sets which result from the EOS program and other elements of Mission to Planet Earth. Currently archived and available for distribution is data from the Earth's Radiation Budget Experiment (ERBE); the International Satellite Cloud Climatology Project (ISCCP); the Stratospheric Aerosol and Gas Experiment (SAGE) ; the Surface Radiation Budget (SRB); the First ISCCP Regional Experiment (FIRE); the Global Tropospheric Experiment (GTE); the Stratospheric Aerosol Measurement (SAM) II; the Aerosol Research Branch (ARB); Measurement of Air

Pollution from Satellites (MAPS); Biomass Burning; NASA Water Vapor Project (NVAP); Nimbus 7 ERB; Scanning Multichannel Microwave Radiometer (SMMR); Smoke/Sulfates, Clouds and Radiation (SCAR) and Subsonic aircraft: Contrail & Clouds Effects Special Study (SUCCESS).

OBTAINING DATA

By following the "Access Data" link on the Langley DAAC home page, users are presented 4 methods for ordering Langley DAAC data.

The Langley DAAC has developed an on-line computer system which allows users to logon, search through the DAAC's data inventory, choose desired data sets, and place an order. Data may be received either electronically (via FTP) or on media such as 4mm tape, 8mm tape, or CD-ROM (prepackaged data sets only). To access follow the "Langley DAAC Order System" link.

For users without x-windows, the new Version 0 WWW Gateway is available. This gateway allows an user to use a WWW browser to search the EOSDIS holdings and order data. Follow the "Multi-DAAC Ordering System (V0 IMS)" to the Version 0 WWW Gateway link.

Orders for prepackaged products available from the Langley DAAC may be placed through the order form for CD-ROMs and Videocassettes. This form is reached through the "Order Form for CD-ROMs and Videocassettes" link.

Selected Langley DAAC products are available for download from the Langley DAAC web site. Follow the "Data Accessible from the Web" link for these data.

HOW TO CONTACT US

For information regarding Langley DAAC data or to place an order, please contact:

Langley DAAC Science, User and Data Support Office
NASA Langley Research Center, Mail Stop 157D
Hampton, VA 23681-0001
Phone: (757) 864-8656 Fax: (757) 864-8807 Internet: larc@eos.nasa.gov

NSCAT will provide an important new tool for weather forecasters to more accurately predict weather, particularly in coastal regions such as Southern California. "Winds over the oceans affect us in Los Angeles directly, because that's where most of our weather comes from," Graf said.

NSCAT has been developed under NASA's strategic enterprise called Mission to Planet Earth, a comprehensive research effort to study Earth's land, oceans, atmosphere, ice and life as an interrelated system. JPL developed, built and manages the NSCAT instrument for NASA. The start of operations initiates a long-term cooperative investigation of Earth by the United States and Japan.

IPCC Technical Paper and Bibliographic Database

Date: 23 April 1997
Organization: University of Michigan

The Intergovernmental Panel on Climate Change (IPCC) Technical Report I: Technologies, Policies and Measures for Mitigating Climate Change is now available online from the US Global Change Research Information Office (GCRIO) at:

http://www.gcrio.org/ipcc/techrepl/toc.html

The report, prepared in response to a request from the UN Framework Convention on Climate Change provides an overview and analysis of technologies and measures to limit and reduce greenhouse gas emissions and to enhance greenhouse gas sinks. In the report technologies and measures are examined over three time periods -- with a focus on the short-(present to 2010) and medium-term (2010-2020), but also including discussion of longer-term (e.g., 2050) possibilities. The Technical Paper includes discussions of technologies and measures that can be adopted in three energy end-use sectors (commercial/residential/institutional buildings, transportation, and industry), as well as in the energy supply sector and the agriculture, forestry, and waste management sectors. Broader measures affecting national economies are discussed in a final section on economic instruments.

The GCRIO, with the assistance of the IPCC Working Group II Technical Support Unit (TSU) has made available a searchable database of all the references used in the three-volume IPCC Second Assessment Report - Climate Change 1995. The references were provided by Cambridge University Press and the database interface allows free-text searches using the citation (title, journal name), searches on the author field, and searches specifying a year or range of years to help narrow the search.

The IPCC Second Assessment Report Bibliographic Database can be accessed under the Showcase Links section of the GCRIO Home Page http://www.gcrio.org

Joe Schumacher, U.S. Global Change Research Information Office
2250 Pierce Rd., University Center MI 48710
Ph: 517-797-2730 Fx: 517-797-2622 http://www.gcrio.org

NSCAT Ocean Wind data available

Date: 25 April 1997
Organization: Jet Propulsion Laboratory - Pasadena CA

NSCAT DATA NOW AVAILABLE VIA FTP

The first batch of NSCAT data (L1.7, L2, L3) is now available via anonymous FTP from podaac.jpl.nasa.gov. It is in the pub/ocean_wind/nscat/ subdirectory. This data has been reprocessed based on the findings of the calibration/validation team. Selected Wind Vector data (25km) will be made available in the next 24 hrs. Batch 25, which covers the time period 19 - 26 February '97, is now available. Batches, which consist of one week of data, will be

added for both the period prior to this and for more recent dates. The users manual and read S/W are also available via FTP. Over the coming weeks the data will be made available on a variety of media. In addition, an NSCAT on-line subsetting routine is soon to be available through the web.

DATA TYPES:

There are currently 5 types of data and, with the exception of the global backscatter data, all of the data is available via FTP. (Level 1.7 is only staged for short periods because of its size.) The data types are produced at different stages in the processing and all but one are "swath data" based on the satellite ground track and are organized in files of one revolution or "rev" each. The one exception is L3 data; a global, daily gridded wind map. All data is geolocated and timetagged. The data is not real-time; the most recent data is about two weeks old. Realtime data will be available through NOAA.

Types of data:
Level 3 - ocean gridded wind map, 0.5 deg. res.
Level 2 - ocean swath wind vectors, 50 km res.
Level 1.7 - ocean-only backscatter, 25 km res.
25 km Dunbar - global backscatter, ocean swath wind vectors, 25 km res.
SWV's - ocean swath Selected Wind Vectors, 25 km res.

DATA PRODUCTS:

The data types have been grouped into products for effective distribution via tape and CD-OM. To obtain a sample of NSCAT data on media other than FTP, place an order through the homepage order form (http://podaac.jpl.nasa.gov/mail-orders.html). (A reminder that much of the data will be available via FTP from podaac.jpl.nasa.gov and does not need to be ordered.)

The three data products are:
085 NSCAT scatterometer ocean wind products CD-ROM (JPL)
(Contains Level 2, 3 and SWV's)
084 NSCAT scatterometer global 25km sigma-0 and ocean winds (Dunbar)
066 NSCAT scatterometer science product, levels 1.7, 2, 3 (JPL)
(Contains Levels 1.7, 2 and 3)

For more information or to order data, please see http://podaac.jpl.nasa.gov or e-mail jpl@eos.nasa.gov.

Data are free of charge.

CERES Pathfinder Data Set Available

Date: 25 April 1997
Organization: NASA Langley Research Center DAAC

EOSDIS RADIATION BUDGET, CLOUDS, AEROSOLS and
TROPOSPHERIC CHEMISTRY DATA

Langley Distributed Active Archive (Langley DAAC)

WWW: http://eosdis.larc.nasa.gov/ e-mail: larc@eos.nasa.gov

The Earth Observing System Data Information System (EOSDIS) Langley Research Center Distributed Active Archive Center (DAAC) announces the release of the Clouds and the Earth's Radiant Energy System (CERES) Pathfinder data. The initial availability of this data is through the Langley DAAC Home Page at http://eosdis.larc.nasa.gov/

This new data set is now available for direct download from the Langley DAAC home page. Follow the "Access Data" link then the "Data Accessible from the Web" link. Follow the "Download Data" link and register to gain access to the CERES Pathfinder data. Note for convenience the data files have been "zipped" to facilitate transfer.

THESE DATA PRODUCTS ARE FREE OF CHARGE.

TYPES OF DATA:
The Langley Distributed Active Archive Center, located in Hampton, Virginia, is responsible for the archival and distribution of NASA science data in the areas of radiation budget, clouds, aerosols and tropospheric chemistry. The Langley DAAC will also archive some of the data sets which result from the EOS program and other elements of Mission to Planet Earth. Currently archived and available for distribution is data from the Earth's Radiation Budget Experiment (ERBE); the International Satellite Cloud Climatology Project (ISCCP); the Stratospheric Aerosol and Gas Experiment (SAGE) ; the Surface Radiation Budget (SRB); the First ISCCP Regional Experiment (FIRE); the Global Tropospheric Experiment (GTE); the Stratospheric Aerosol Measurement (SAM) II; the Aerosol Research Branch (ARB); Measurement of Air Pollution from Satellites (MAPS); Biomass Burning; NASA Water Vapor Project (NVAP); Nimbus 7 ERB; Scanning Multichannel Microwave Radiometer (SMMR); Smoke/Sulfates, Clouds and Radiation (SCAR) and Subsonic aircraft: Contrail & Clouds Effects Special Study (SUCCESS) .

HOW TO CONTACT US

For information regarding Langley DAAC data or to place an order, please contact:

Langley DAAC Science, User and Data Support Office
NASA Langley Research Center, Mail Stop 157D
Hampton, VA 23681-0001
Phone: (757) 864-8656 Fax: (757) 864-8807 Internet: larc@eos.nasa.gov

CONSEQUENCES Vol. 3, No. 1 available

Date: 2 May 1997
Organization: University of Michigan

The US Global Change Research Information Office (GCRIO) is pleased to announce that the latest issue of CONSEQUENCES: The Nature and Implications of Environmental Change is now online.

This first issue of CONSEQUENCES Volume 3 contains review articles entitled, "The Case of the Missing Songbirds" by Scott K. Robinson, ornithologist at the Center for Wildlife Ecology of the Illinois Natural History Survey; and "Do We Still Need Nature? The Importance of Biological Diversity" by Anthony C. Janetos, ecologist with NASA's Mission to Planet Earth.

All issues of CONSEQUENCES may be accessed at:

http://www.gcrio.org/CONSEQUENCES/introCON.html

Joe Schumacher, U.S. Global Change Research Information Office
2250 Pierce Rd., University Center MI 48710
Ph: 517-797-2730 Fx: 517-797-2622 http://www.gcrio.org

Bill Kyle

Department of Geography & Geology, The University of Hong Kong
Pokfulam Road, Hong Kong (Email: billkyle@hkusua.hku.hk)

Hong Kong Weather Reviews

Climatological information employed in the compilation of this section is derived mainly from published weather data of the Hong Kong Observatory and is used with the prior permission of the Director.

Review of Autumn 1996

Seasonal statistics

Mean daily maximum temperature	27.8 °C	(0.3 °C above normal)
Mean daily temperature	25.6 °C	(0.9 °C above normal)
Mean daily minimum temperature	23.6 °C	(1.0 °C above normal)
Rainfall (provisional)	652.3 mm	(136 %)

September

September 1996 was wetter than normal. The total monthly rainfall of 604.0 mm was more than twice the normal figure of 299.7 mm and the sixth highest on record for the month. Two tropical cyclones, Sally and Willy necessitated the hoisting of tropical cyclone signals.

The month started fine with light winds on the first day. It was hazy in the morning the next day, but then the weather became cloudy with isolated thunderstorms in the afternoon. Winds turned easterly on 3rd and isolated thunderstorms continued to affect the territory until the early morning of 5th. Fine and sunny weather returned later that morning. Generally sunny weather then prevailed for the next two days and the temperature rose to 33.0°C on 8th, the

highest recorded during the month. Meanwhile, over the Philippine Sea about 1,300 km east of Manila, tropical depression Sally formed on 5th. It moved west-northwestwards and intensified over the warm water to attain typhoon strength on 7th. Sally entered the South China Sea on the morning of 8th prompting the hoisting of the Stand By Signal No. 1 at 0500 HKT that day when Sally was about 770 km to the southeast of the territory. At that time local winds were light gradually becoming moderate northeasterly. Sally was a particularly fast moving typhoon crossing in a west-northwesterly track across the northern part of the South China Sea at an average speed of 38 km h^{-1}. As Sally moved closer to Hong Kong the Strong Wind Signal No. 3 was raised at 1700 HKT. Winds strengthened rapidly that evening as the outer rainbands of the storm brought thundery and frequent squally showers to Hong Kong. Sally was closest to Hong Kong around 0200 HKT on 9th when it was about 180 km to the south. The Royal Observatory recorded the lowest hourly sea level pressure of 100.00 kPa at this time. From then on winds veered from northeasterly to southeasterly resulting in an increase in wind speed in Victoria Harbour to gale force. Consequently the SE Gale or Storm Signal No.8 was hoisted at 0215 HKT. Gale force winds with maximum hourly speed of 96 km h^{-1} were recorded at Waglan Island at 0100 HKT and of 88 km h^{-1} on Cheung Chau at 0400 HKT on 9th. Within the harbour, at Green Island, King's Park and Star Ferry, maximum gust exceeding 100 km h^{-1} were also recorded during these few hours. However, as Sally continued to move rapidly away the SE Gale or Storm Signal No. 8 was replaced by the Strong Wind Signal No. 3 at 0540 HKT as gales began to subside. The No. 8 signal was hoisted for only 3 hours and 25 minutes, the shortest time period since 1984. All signals were lowered at 1015 HKT on 9th. Locally, there was relatively minor damage although two persons were killed and two others reported injured during the passage of Sally. As the storm moved away from the territory the weather improved rapidly and generally fine weather prevailed on 10th and 11th. Easterly winds freshened later that day with the development of an area of low pressure over the northern part of the South China Sea. The next day was cloudy with isolated showers. These became more frequent, heavy and thundery on 13th. With the continuing disturbed weather, the third highest daily total rainfall for September, 227 mm, was recorded on 14th. Temperatures also dropped to the lowest for the month, 23.6°C, on that day. The heavy rain resulted in eight landslips and 24 flooding incidents. One landslip, requiring the evacuation of 43 residents, occurred in Tai Hang Road. The next day continued windy and rainy but both then subsided and the weather became generally fine again on 16th and 17th. On the morning of 18th Tropical Depression Willie formed about 200 km west-northwesrt of Xisha and intensified into a tropical storm later that afternoon. At first it moved northeastwards but adopted a more northwesterly track the next day as it intensified into a severe tropical storm. The Stand By Signal No. 1 was hoisted at 2315 HKT on 18th when Willie was about 470 km to the south-southwest. Willie was closest to the territory on the afternoon of 19th when it was about 390 km to the southwest. The Royal Observatory recorded lowest hourly sea level pressure of 100.24 kPa at both 1500 and 1600 HKT that day. Willie continued to turn more westerly and then west-southwesterly as it passed between Hainan Dao and Leizhou Peninsula taking it away from the territory. The No. 1 signal was lowered at 0900 HKT on 20th. While the signal was hoisted local winds were moderate easterly. However, from 19th to 22nd heavy and thundery showers associated with the outer rainbands of Willie affected the territory. Rain was heaviest in the northeast where widespread flooding was reported in Sha Tau Kok and Ta Kwu Ling. The weather remained generally cloudy with some showers on 23rd. Strong easterly winds affected offshore areas on 24th. Some isolated heavy showers occurred over Hong Kong Island on 27th. With winds turning more northerly the next day the weather became fine and sunny . The fine conditions prevailed until the end of the month although there were some brief showers on 30th.

Monthly Statistics

Extreme daily maximum temperature	33.0 °C	(on 8th)
Mean daily maximum temperature	29.9 °C	(0.4 °C below normal)
Mean daily temperature	27.7 °C	(0.1 °C above normal)
Mean daily minimum temperature	25.7 °C	(0.2 °C above normal)
Extreme daily minimum temperature	23.6 °C	(on 14th)
Total Rainfall (provisional)	604.0 mm	(202 % of normal)
Number of Days with ≥0.1 mm rain	19	(4.63 above normal)
Number of Days with ≥25.0 mm rain	7	(3.43 above normal)
Number of Days with ≥50.0 mm rain	3	(1.37 above normal)

October

October 1996 was warmer and drier than normal. The mean temperature of 26.0°C was the sixth highest on record for the month. The mean minimum temperature of 24.0°C was the seventh highest. A total of only 44.8 mm of rain was recorded, 100 mm less than the normal figure of 144.8 mm. One tropical cyclone, Beth, affected the territory and necessitated the hoisting of the Stand By No. 1 Tropical Cyclone Signal. Fire Danger Warnings were issued three times during the month.

There were some light showers but also sunny periods on the first day of the month. Some light showers fell again in the afternoon of the following day. It was fine but hazy on 3rd and the weather remained fine for the next few days although there were some isolated heavy showers in the eastern New Territories on the morning of 6th. Temperatures reached the maximum recorded for the month, 30.3°C, on a fairly hot afternoon the next day. A weak cold front crossed the coast of South China early in the morning of 8th. Behind this cold front the northerlies brought slightly cooler weather and some showers to the territory. However, the effect was short-lived and generally fine weather returned and persisted for the following few days. During this time the Yellow Fire Danger Warning was issued from 0630 HKT on 12th to 1730 HKT on 13th. Cloudy weather and light rain returned on 14th and 15th as an area of low pressure over the northern part of the South China Sea brought an enhancement of the northeast monsoon over the coastal areas. The disturbed weather did not last long and it turned sunny again on 16th. In the mean time a tropical depression named Beth developed over the Philippine Sea about 970 km east-northeast of Manila on 15th. The depression tracked westwards towards northern Luzon reaching tropical storm status the next day and typhoon status on 17th. Beth made landfall on Luzon late that day, crossed the island and entered the South China Sea on 18th. As Beth moved closer to Hong Kong, the combined effect of the storm and a strengthening monsoon resulting in strengthening of winds over the territory. This resulted in the Yellow Fire Danger Warning being issued for the second time

from 0600 HKT on 19th to 1640 HKT on 20th. The Tropical Cyclone Stand By Signal No. 1 was hoisted at 1145 HKT on 19th when Beth was about 560 km to the southeast. Beth had a small circulation and also weakened rapidly as it traversed the South China Sea under the impact of the strengthening monsoon. As a consequence Hong Kong was not seriously affected by her passage apart from rain on 20th brought by the outer rainbands of the storm. That day was the wettest in the month with 22.2 mm, nearly half the monthly total, being recorded at the Royal Observatory. The cloudy skies and damp conditions also resulted in the lowering of temperatures to the month's minimum of 20.5°C. Beth was closest to Hong Kong around 0500 HKT on 20th when it was about 470 km to the south-southeast. However, the Royal Observatory recorded the lowest hourly sea level pressure of 101.09 kPa at 1500 HKT the previous day, some 14 hours earlier when Beth was more vigorous. As Beth weakened and drifted further away the No. 1 signal was lowered at 1400 HKT on 20th. Although there was some rain on 21st the weather improved and remained fine from 22nd to 25th. Winds freshened from the north the next day bringing cool, dry conditions. These dry conditions resulted in the Red Fire Danger Warning being issued from 1100 HKT on 25th to 1800 HKT on 27th. As winds turned easterly generally fine weather continued from 27th until the end of the month.

Monthly Statistics

Extreme daily maximum temperature	30.3 °C	(on 7th)
Mean daily maximum temperature	28.2 °C	(0.3 °C above normal)
Mean daily temperature	26.0 °C	(0.8 °C above normal)
Mean daily minimum temperature	24.0 °C	(0.9 °C above normal)
Extreme daily minimum temperature	20.5 °C	(on 20th)
Total Rainfall (provisional)	44.8 mm	(31 % of normal)
Number of Days with ≥0.1 mm rain	8	(0.60 below normal)
Number of Days with ≥25.0 mm rain	0	(1.50 below normal)
Number of Days with ≥50.0 mm rain	0	(0.40 below normal)

November

November 1996 was, like the previous month, warmer and drier than normal. The mean minimum temperature of 21.1°C was highest ever recorded for November. The mean temperature and mean maximum temperature of 23.0°C and 25.3C were the second and seventh highest respectively for the month. The winter monsoon flow was not well developed as evidenced by the fact that the monthly mean sea-level pressure of 101.58 kPa was the sixth lowest on record. Cold continental air thus affected the area less frequently than normal and the Strong Monsoon Signal had to be raised on only three occasions. Only 3.5 mm of rain was recorded for the whole of the month compared to a normal of 35.1 mm for the 1961-90

period. Owing to the generally dry conditions Fire Danger Warnings, six Yellow and two Red, had to be issued during the month.

Fine and sunny weather on the first day of November brought the maximum temperature that afternoon to the highest recorded for the month of 29.8°C. However, a cold front reached the coast of South China on 2nd, with easterly winds strengthening and some light rain patches during the night. The Yellow Fire Danger Warning was issued from 0645 to 1800 HKT on that day. Winds strengthened that afternoon necessitating the hoisting of the Strong Monsoon Signal at 1420 HKT. Strong winds continued on 3rd resulting in the issuance of the Yellow Fire Danger Warning again from 0830 to 1800 HKT that day. The winds subsided the next day and the Strong Monsoon Signal was lowered at 1030 HKT on 4th. Fine weather then prevailed for the next four days. Northerly winds returned from 9th resulting in the issuance of the Yellow Fire Danger Warning from 0600 HKT on that day until 0600 HKT on 11th even though light rain patches affected the territory during this time. The combined effect of the strengthening of the winter monsoon over China and the presence of Tropical Depression Ernie over the northern part of the South China Sea led to a strengthening of winds locally on the evening of 13th. The Strong Monsoon Signal was hoisted overnight from 0130 to 0530 HKT on 14th. The clouds cleared on that day but returned again on 15th. Some light rain patches also occurred on 16th. Another dry, northerly surge of the winter monsoon arrived on 17th and winds were strong offshore that and the following day with the Strong Monsoon Signal hoisted from 1930 HKT on 17th to 1135 HKT on 18th. The minimum temperature recorded on the morning of 18th, 16.3°C, was the lowest for the month. The generally dry and windy conditions also resulted in the issuance of the Yellow Fire Danger Warning from 0600 to 1720 HKT on 17th and its replacement by the Red Fire Danger Warning from that time until 0600 HKT on 22nd. During this time winds gradually turned to the east on 20th. Easterly winds and generally fine conditions prevailed from 21st to 29th. The Red Fire Danger Warning was issued again from 1035 HKT on 22nd to 0600 on 23rd at which time it was replaced by the Yellow Fire Danger Warning until 1800 HKT on 24th. A cold front crossed the south China coast on the afternoon of 29th bringing drier and cooler winds from the north on the last day of the month. The Yellow Fire Danger Warning was issued for the last time in November from 0600 HKT on 30th to 0545 HKT on 1st December.

Monthly Statistics

Extreme daily maximum temperature	29.8 °C	(on 1st)
Mean daily maximum temperature	25.3 °C	(1.1 °C above normal)
Mean daily temperature	23.0 °C	(1.6 °C above normal)
Mean daily minimum temperature	21.1 °C	(1.9 °C above normal)
Extreme daily minimum temperature	16.3 °C	(on 18th)
Total Rainfall (provisional)	3.5 mm	(10 % of normal)
Number of Days with ≥0.1 mm rain	5	(0.87 above normal)
Number of Days with ≥25.0 mm rain	0	(0.40 below normal)

Number of Days with ≥50.0 mm rain	0	(0.10 below normal)

Daily maximum temperature trends

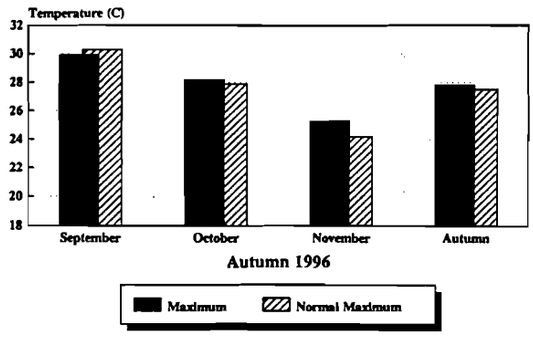

Daily mean temperature trends

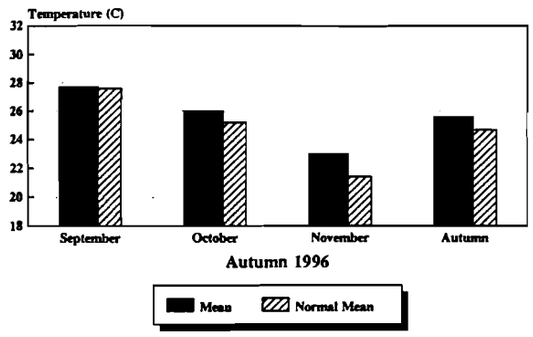

Daily minimum temperature trends

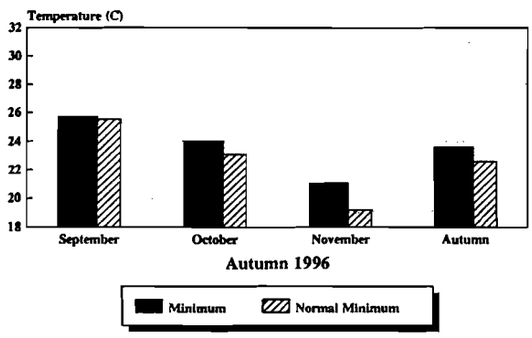

Rainfall trends

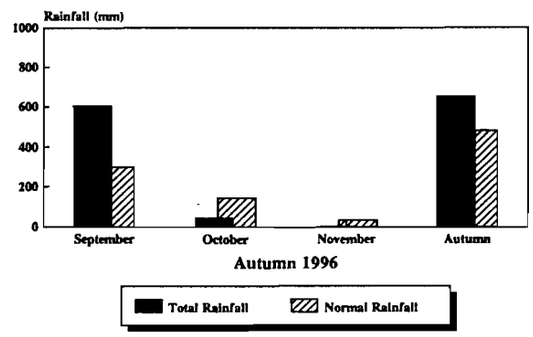

Review of Winter 1996-97

Seasonal statistics

Mean daily maximum temperature	19.1 °C	(0.2 °C below normal)
Mean daily temperature	17.1 °C	(0.6 °C above normal)
Mean daily minimum temperature	15.3 °C	(1.0 °C above normal)
Rainfall (provisional)	156.3 mm	(158 %)

December

December 1996 was generally fine and very dry. Only a trace of rainfall was recorded compared to a normal amount of 27.3 millimetres. The dry conditions were reflected in the low mean relative humidity of 64 percent (4 percent below normal) and the fact that Fire Danger Warnings (six Yellow and eight Red)were in effect for 27 days during the month. The fine conditions were the result of a preponderance of dry continental airstreams affecting the south China coastal area. As a consequence the mean temperature and mean minimum temperature of 18.3°C and 16.4°C were respectively 0.7 °C and 1.0 °C higher than the normal values for the 1961-90 period.

The first day of December was fine and sunny although cloud increased that evening as easterly winds began to dominate. The Yellow Fire Danger Warning which was issued at 0600 HKT on 30 November was replaced at 0545 HKT by the Red Fire Danger Warning at 0545 HKT on that day. Winds became strong offshore early the next morning necessitating the hoisting of the Strong Monsoon Signal at 0315 HKT on 2nd although it was lowered at 0745 HKT as winds eased. Some light rain patches that evening produced a trace of rainfall, the first of only two occasions when traces of rain were registered at the Observatory during the month. During the next two days the continental anticyclone intensified and a cold front reached the south China coast on the morning of 5th bringing drier air and resulting in the issuance of the Red Fire Danger Warning at 1800 HKT and the hoisting of the Strong Monsoon Signal at 2025 HKT that day. As winds eased the Monsoon Signal was lowered at 0925 HKT the next morning. However, the Red Fire Danger Warning remained in force until 1730 HKT on 9th as dry conditions continued to prevail. During this time winds strengthened from the north on 6th and temperatures dropped to 13.5°C, the lowest recorded for the month. Easterly winds returned on the afternoon of 7th and it became cloudy. A dry continental airstream reached Hong Kong on 9th, clearing the clouds the next day and resulting in the issuance of the Red Fire Danger Warning again at 0600 HKT on 10th, only 12 and a half hours after it had been lowered after being in force for nearly four days. During the next week weather remained generally fine and dry with long, sunny periods. During this time the Red Fire Danger Warning was withdrawn at 0600 HKT on 12th, only to be re-issued at 0600 HKT on 13th and replaced by the Yellow Fire Danger Warning from 0600 HKT on 14th until 0600 HKT on 16th. The generally fine and sunny weather conditions during this time culminated in a maximum temperature of 24.8°C on the afternoon of 17th, the highest temperature recorded during the month. That evening a surge of the winter monsoon reached the south China coast and winds freshened offshore. Drier air affecting Hong Kong again necessitated the issuance of the Red Fire Danger Warning at 0000 HKT on 18th. Temperatures dropped about three degrees that day but increasing humidity resulted in the replacement of the Red with the Yellow Fire Danger Warning at 1800 HKT. It was cloudy and hazy the following day but sunny conditions returned on 20th. Fine weather with varying cloud continued until Christmas Day with the Red Fire Danger Warning replacing the Yellow at 0600 HKT on 21st, the Yellow being reissued again at 0600 HKT the next day, only to replaced once more by the Red at 0600 HKT on 23rd. This alternating sequence of issuing Red and Yellow Fire Danger Warnings continued as the Red was replaced by the Yellow at 1730 HKT on 23rd, the Red reissued at 0600 HKT on 24th, to be replaced once again by the Yellow at 1730 HKT on Christmas Eve. A few light rain patches again occurred on 26th resulting in the second recorded trace of rain at the Observatory. Otherwise fine weather with sunny periods during the day prevailed for the rest of the month although some cloud was observed on 29th. The Yellow fire danger warning was finally withdrawn at 0730 HKT on 30th.

Extreme daily maximum temperature	24.8 °C	(on 17th)
Mean daily maximum temperature	20.4 °C	(0.1 °C below normal)
Mean daily temperature	18.3 °C	(0.7 °C above normal)
Mean daily minimum temperature	16.4 °C	(1.0 °C above normal)
Extreme daily minimum temperature	13.5 °C	(on 6th)
Total Rainfall (provisional)	0.0 mm	(0 % of normal)
Number of Days with ≥0.1 mm rain	0	(3.87 below normal)
Number of Days with ≥25.0 mm rain	0	(0.23 below normal)
Number of Days with ≥50.0 mm rain	0	(0.10 below normal)

January

Generally speaking, January 1997 was sunnier, warmer and wetter than the longterm average conditions. The monthly mean temperature of 16.7°C and total rainfall of 44.6 millimetres were 0.9°C and 21.2 millimetres higher than the normal figures of 15.8°C and 23.4 millimetres respectively. The mean daily minimum temperature of 14.7°C was also 1.1°C warmer than the 30-year normal. In the case of rainfall the amount was nearly double the normal value. Similarly, the total sunshine recorded during the month was 173.6 hours, 21.2 hours higher than the 1961-90 normal amount. Despite the generally humid conditions, nine Yellow and five Red Fire Danger Warnings were issued during the month.

The fine and sunny weather at the end of 1996 continued into 1997. The Yellow Fire Danger Warning was issued at 0600 HKT on 1st, was replaced by the Red at 0615 HKT on 2nd, and the latter was rescinded at 1220 HKT the same day as it turned cloudy and rainy as winds freshened from the east. The wind changed to northerly gradually the next evening and rain eased off on 4th. A weak cold front crossed the south China coast on 5th bringing fresh northerly winds and drier air to clear the clouds. As a result the Yellow Fire Danger Warning was issued at 0600 HKT that morning. Winds became easterly on 6th January while the weather remained fine and dry for the next few days. The Yellow Fire Danger Warning was replaced by the Red at 0600 HKT on 6th but this was changed back to Yellow at 1800 HKT that evening. During this time a hill fire broke out in Fei Ngo Shan on 7th and lasted for 15 hours. Trees in an area of 0.36 million square metres were destroyed. A replenishment of the winter monsoon reached the south China coastal area on 8th and the Red Fire Danger Warning was again issued at 0600 HKT that day although it was replaced by the Yellow Fire Danger Warning at 1730 HKT. This latter warning remained in force until 1800 HKT on 10th when it was again replaced by the Red Warning at that time. The weather remained fine and dry until 12th when easterly winds returned and the Yellow Fire Danger Warning replaced the Red once again at 0600 HKT that day. Cloudy conditions set in and there were light rain patches on 14th so that the Yellow Warning was rescinded at 0600 HKT that day. After the passage of a weak cold front on 15th, the weather became fine and sunny during the day. Another weak cold

front brought along generally cloudy conditions again on 18th. It was misty or hazy at times inside the harbour during the next couple of days. Despite this the Yellow Fire Danger Warning was again issued from 0600 to 1800 HKT on 19th. The weather became overcast with rain patches late on 21st. Meanwhile, an intense cold front formed over China and moved southwards. In anticipation of strengthening winds the Strong Monsoon Signal was hoisted at 2300 HKT on 21st. Winds strengthened from the east early on 22nd and as a result a cargo vessel capsized near the Ninepin Group although fortunately all crewmen were rescued. In addition, a scaffolding collapsed in Lam Tin and a sign board in Jordan was blown down in strong winds injuring one person. The Strong Monsoon Signal was lowered at 0630 HKT on 23rd as winds subsided. The cold front crossed the coast of Guangdong later on 23rd with squally showers affecting Hong Kong. Temperatures dropped a few degrees in one hour. Strengthening winds resulting in the hoisting of the Strong Monsoon Signal again that evening at 2115 HKT although it was lowered at 1000 HKT the next morning. A minimum temperature of 10.2 °C, the lowest in the month, was recorded on both 24th and 25th. Drier air from the north resulted in the issuance of the Yellow Fire Danger Warning from 0800 to 1615 HKT on 24th and again at 0605 HKT on 25th. This dry air cleared the clouds gradually the following day but led to conditions which required the replacement of the Yellow Fire Danger Warning by the Red at 0600 HKT on 27th. The return of moister conditions saw the Red being replaced by the Yellow Fire Danger Warning once again at 0600 HKT on 29th. Apart from some cloudy periods on 30th, fine and dry weather prevailed until the end of the month. Temperatures rose to 23.9 °C, the highest recorded during the month, on 31st although the Yellow Fire Danger Warning was rescinded at 0600HKT that day.

Extreme daily maximum temperature	23.9 °C	(on 31st)
Mean daily maximum temperature	18.9 °C	(0.3 °C above normal)
Mean daily temperature	16.7 °C	(0.9 °C above normal)
Mean daily minimum temperature	14.7 °C	(1.1 °C above normal)
Extreme daily minimum temperature	10.2 °C	(on 24th and 25th)
Total Rainfall (provisional)	44.6 mm	(191 % of normal)
Number of Days with ≥0.1 mm rain	6	(0.37 above normal)
Number of Days with ≥25.0 mm rain	1	(0.90 above normal)
Number of Days with ≥50.0 mm rain	0	(normal)

February

February 1997 was, like January, also wetter and warmer than normal although, unlike January, it was also less sunny. The monthly total rainfall of 111.7 millimetres was 63.7 millimetres higher than the normal figure of 48.0 millimetres. The total sunshine duration in

the month of 85.5 hours was 12.2 hours lower than normal. The wet conditions also meant that only three Yellow and two Red Fire Danger Warnings were issued during the month.

The month began with strong easterly winds and increasing cloud amount under the influence of an intense winter monsoon. The Strong Monsoon Signal was hoisted between 0245 and 0750 HKT on 1st. However, winds gradually subsided during the day and there were light rain patches. The next day, rain became heavy with squally thunderstorms necessitating the issuing of the Thunderstorm Warning overnight from 2110 HKT on 2nd to 0800 HKT on 3rd. The passage of a cold front resulted in the hoisting of the Strong Monsoon Signal from 0250 to 1800 HKT on 3rd as easterly winds strengthened again and rainy conditions continued. The weather improved temporarily on 4th but there patches of rain again the next day. Easterly winds strengthened late on 6th and the Strong Monsoon Signal was again hoisted from 0015 to 0630 HKT on 7th. However, the easterlies were soon replaced by moderate northerlies. The weather remained generally cloudy with periods of light rain easing off gradually on 8th. Northerly winds and cloud conditions then continued. On 12th, winds freshened from the east bringing periods of rain. Strong easterly winds affected the offshore areas early on 14th and the Strong Monsoon Signal was hoisted for the fourth and last time during the month from 0010 to 1015 HKT that day. The weather remained overcast, but winds moderated and turned northerly the next day. A drier airstream reached the south China coastal areas on 18th with the lowest temperature in the month, 10.9 °C, being recorded that morning. As dry air continued to come from the northeast, clouds cleared and the weather became fine and sunny on 19th. As a consequence the Yellow Fire Danger Warning was issued at 0600 HKT on 19th. Fine weather prevailed for the next 5 days until a maritime airstream set in bringing warm weather to the territory on 24th. During this time the Red Fire Danger Warning was in force from 0600 HKT on 20th to 0600 HKT on 21st and again from 0600 HKT on 22nd to 1800 HKT on the same day, and the Yellow Fire Danger Warning was in place from 0600 HKT on 21st to 0600 HKT on 22nd and from 1800 HKT on the same day to 1800 HKT the next day. Apart from a few light rain patches early on 25th, the weather remained fine until the end of the month. During this fine spell temperatures rose to 24.6 °C, the maximum recorded for the month, on 26th.

Extreme daily maximum temperature	24.6 °C	(on 26th)
Mean daily maximum temperature	18.0 °C	(0.6 °C below normal)
Mean daily temperature	16.1 °C	(0.2 °C above normal)
Mean daily minimum temperature	14.6 °C	(0.7 °C above normal)
Extreme daily minimum temperature	10.9 °C	(on 18th)
Total Rainfall (provisional)	111.7 mm	(233 % of normal)
Number of Days with ≥0.1 mm rain	11	(2.07 above normal)
Number of Days with ≥25.0 mm rain	2	(1.57 above normal)
Number of Days with ≥50.0 mm rain	0	(0.03 below normal)

Daily maximum temperature trends

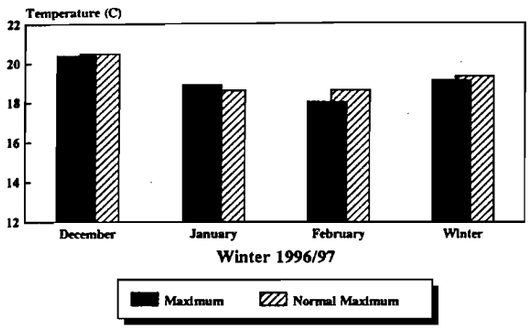

Daily mean temperature trends

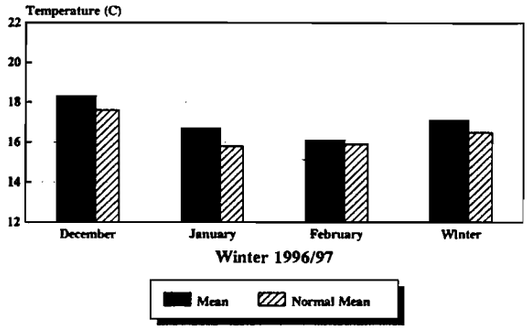

Daily minimum temperature trends

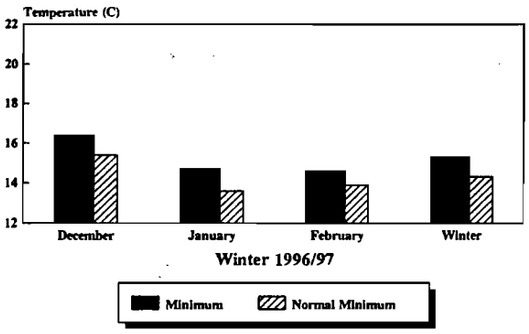

Rainfall trends

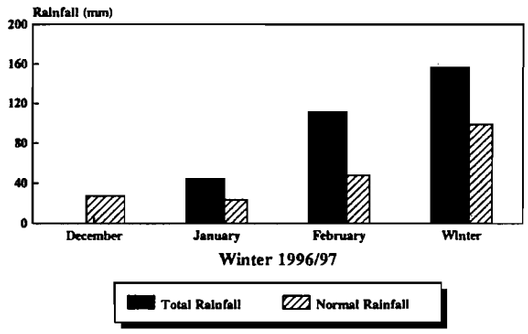

HONG KONG METEOROLOGICAL SOCIETY

INFORMATION FOR CONTRIBUTORS TO THE BULLETIN

Technical or research articles, as well as reviews and correspondence of a topical nature are welcome. In general contributions should be short, although exceptions may be made by prior arrangement and at the sole discretion of the Editorial Board. Copyright of material submitted for publication remains that of the author(s). However, any previous, current, or anticipated future use of such material by the author must be stated at the time of submission. All existing copyright materials to be published must be cleared by the contributor(s) prior to submission.

Manuscripts must be accurate and preferably in the form of a diskette containing an electronic version in one of the common word processing formats. WORD is preferred but others are also acceptable. Whether or not an electronic version is submitted, two complete manuscript copies of the articles should be submitted. These should be preceded by a cover page stating the title of the article, the full name(s) of the author(s), identification data for each author (position and institution or other affiliation and complete mailing address). An abstract of about 150 words should be included. Manuscripts should be double-spaced, including references, single-side only on A4 size paper with a 2.5 cm margin on all sides, and be numbered serially. All references should be arranged in alphabetical and, for the same author, chronological order. In the text they should be placed in brackets as (Author'(s) name(s), date). In the reference list at the end the Author'(s) name(s) and initials followed by the date and title of the work. If the work is a book this should be followed by the publisher's name, place of publication and number of pages; or, if a journal article, by the title of the periodical, volume and page numbers.

Submission of electronic versions of illustrations is encourage. Originals of any hardcopy illustrations submitted should be in black on tracing material or smooth white paper, with a line weight suitable for any intended reduction from the original submitted size. Monochrome photographs should be clear with good contrasts. Colour photographs are also accepted by prior arrangement with the Editorial Board. Originals of all illustrations should be numbered consecutively and should be clearly identified with the author'(s) name(s) on the back. A complete list of captions printed on a separate sheet of paper.

All submitted material is accepted for publication subject to peer review. The principal author will be sent comments from reviewers for response, if necessary, prior to final acceptance of the paper for publication. After acceptance the principal author will, in due course, be sent proofs for checking prior to publication. Only corrections and minor amendments will be accepted at this stage. The Society is unable to provide authors with free offprints of items published in the Bulletin, but may be able to obtain quotations from the printer on behalf of authors who express, at the time of submission of proofs, a desire to purchase a specified number of offprints.

Enquiries and all correspondence should be addressed to the Editor-in-Chief, Hong Kong Meteorological Society Bulletin, c/o Department of Geography & Geology, The University of Hong Kong, Pokfulam Road, Hong Kong. (*Tel. +(852) 2859-7022; Fax. +(852) 2559-8994 or 2549-9763; email: billkyle@hkusua.hku.hk or billkyle@hkucc.hku.hk.*

香港氣象學會

HONG KONG METEOROLOGICAL SOCIETY

Bulletin

VOLUME 7, NUMBER 1, 1997

SINGLE COPY PRICE: HK$ 150

(for subscription rates see inside front cover)

CONTENTS